THE ELECTRONIC BAND STRUCTURE OF VANADIUM OXIDE (VO)

D. J. KRAAN

THE ELECTRONIC BAND STRUCTURE OF VANADIUM OXIDE (VO)

PROEFSCHRIFT

TER VERKRIJGING VAN DE GRAAD VAN DOCTOR IN DE TECHNISCHE WETENSCHAPPEN AAN DE TECHNISCHE HOGESCHOOL DELFT, OP GEZAG VAN DE RECTOR MAGNIFICUS IR. H. B. BOEREMA, HOOGLERAAR IN DE AFDELING DER ELEKTROTECHNIEK, VOOR EEN COMMISSIE AANGEWEZEN DOOR HET COLLEGE VAN DEKANEN TE VERDEDIGEN OP WOENSDAG 27 FEBRUARI 1974 TE 16.00 UUR

DOOR

DIRK JAN KRAAN

SCHEIKUNDIG INGENIEUR
GEBOREN TE ROTTERDAM

1974
IMPRIMERIE DEROUAUX – LIÈGE

DIT PROEFSCHRIFT IS GOEDGEKEURD DOOR DE PROMOTOR

PROF. DR. IR. L. L. VAN REIJEN

Aan mijn ouders

A mon épouse Lucie

C O N T E N T S

CHAPTER I - INTRODUCTION

The semiconductor-to-metal transition has been the subject of many studies for several years. Under the compounds that show such a transition are the vanadium oxides. Morin (1) was the first to establish the semiconductor-to-metal transition of some vanadium oxides. His conductivity measurements are summarized in figure 1.1. Besides the jump in conductivity, Morin (1) also found

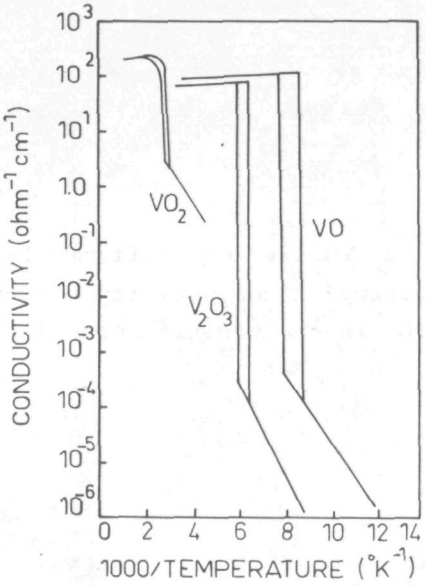

Fig. 1.1 Conductivity vs. T curves of some vanadium oxides. *

a transition point for the magnetic susceptibility and specific heat curves. Since Morin, many other research workers have established the semiconductor-to-metal transition of the vanadium oxides. Some characteristic data are given in figures 1.2 and 1.3.

A special point of discussion is vanadium monoxide, which has the NaCl structure (figure 1.4). Experimental results on the conductivity of this compound have often been in contradiction with each other. Moreover, no transition points have been observed for magnetic susceptibility and specific heat.

Just like Morin, Austin (5) found that the conductivity jumped by a factor of 10^6 at about $T_0 = 126\ ^oK$. In later years the

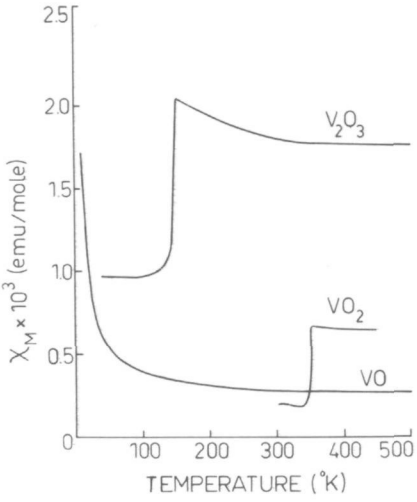

Fig. 1.2 Magnetic susceptibility vs. T curves of resp. VO (ref.8), V_2O_3 (ref.2) and VO_2 (ref.3).

semiconductor-to-metal transition of fcc VO has been affirmed by the work of Warren *et al.* (6), who observed a conductivity discontinuity of greater than a factor of 10^4 in the vicinity of 125 °K.

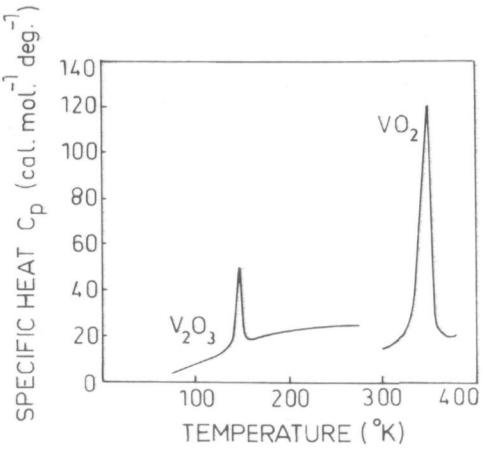

Fig. 1.3 Specific heat vs. T curves of resp. V_2O_3 (ref.4) and VO_2 (ref.3).

However, contrary to these results are the observations of Kawano *et al.* (7), who measured the conductivity of samples of VO over a temperature range of 100-250 °K and found no transition.

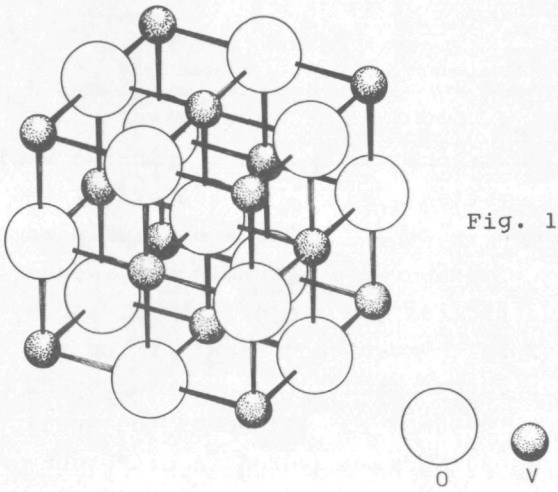

Fig. 1.4 The rocksalt structure of VO.

The same conclusion has been drawn by Banus *et al.* (8), Takei *et al.* (9) and Honig *et al.* (10,11). Although this last group of research workers concludes that VO does not show a semiconductor-to-metal transition, their numerical results deviate. For example, the conductivity σ at 300 ^{o}K varies from 5×10^{2} $\Omega^{-1}cm^{-1}$ (7,9-11) to 14×10^{2} $\Omega^{-1}cm^{-1}$ (8). Takei *et al.* (9) report that no marked change in the conductivity has been observed in the temperature region of 77-300 ^{o}K. This is a contrast with the other experimentalists, who mention an increase in conductivity with increasing temperature.

χ measurements, too, have been performed for VO. Like the electric data, the magnetic data (susceptibility vs. T curves) are not at all of the same tenor. The 15% randomly distributed vacancies in VO disturb the lattice periodicity, which makes the solid actually a disordered material. According to Anderson's theory (12) both collective and localized electrons can be present. This must be reflected by the formula for χ, which is therefore proposed to be:

$$\chi = \chi_0 + C/(T+\theta)$$

The second term signifies the Curie-Weiss law, while χ_0 is com-

posed of a sum of several contributions:

$$\chi_0 = \chi_{ion} + \chi_{sp} + \chi_L + \chi_{VV}$$

while χ_{ion} is the diamagnetism of the ion cores, χ_{sp} is the Pauli paramagnetism of the conduction electrons, χ_L is the associated Landau diamagnetism and χ_{VV} denotes the Van Vleck orbital paramagnetic term. The parameters χ_0, C and θ are determined by measuring the susceptibility χ as a function of the temperature T, and applying a least-squares procedure to have an optimal fit of the experimental values to the above proposed formula. A survey of these χ measurements is shown in table 1.1. Although the susceptibility data of the first three authors, measured in different ranges of temperatures, fit together reasonably well, the derived magnetic moments show rather large deviations. μ_{eff} is extracted from the variable C ($\mu_{eff} = 2.2\times10^{12}\sqrt{C/N}$, N is Avogadro's number), it is a measure for the number of paramagnetic cations that have localized orbitals. In the border-line case that all vanadium ions

Table 1.1

Survey of the χ measurement results on VO

	$\chi_0\times10^4$ (emu/mole)	$C\times10^2$ (emu)	θ (^oK)	μ_{eff}	Temp. range (^oK)
Banus *et al.* (8)	2.3	1.6	1.4	0.36	4 - 300
Massard *et al.* (13)	2.5	6.0	112	0.69	80 - 900
Suzuki *et al.* (14)	1.5	5.9	-	0.69	100 - 300
Aivazov *et al.* (15)	0.15	14.9	176	1.09	100 - 250
	0.11	66.9	1530	2.32	250 - 850

have non-interacting localized orbitals, μ_{eff} will be 3.87 ($\mu_{eff} = \sqrt{n(n+2)}$, n is the number of unpaired electrons). The experimental data of μ_{eff} are considerably lower. Hence a description of VO as a paramagnetic compound with localized magnetic moments does not seem relevant. The variable θ is a measure for the interaction between the paramagnetic cations and becomes larger as μ_{eff} becomes larger. Suzuki *et al.* (14) used the Curie law, instead of the Curie-Weiss law, which implicates that θ is actually zero. We establish further that Aivazov *et al.* (15) found a transition in the χ vs. T curve at $T_0 = 250\ ^{o}K$, as contrasted with the other authors. Suzuki *et al.* (14), as opposed to the others, determined χ_{VV} by measuring the Knight shift of ^{51}V in the VO crystal. According to their experiments, χ_{VV} equals 1.12×10^{-4} emu/mole, which is already some factors larger than Aivazov's χ_0 values. χ_L is a negligible quantity, while χ_{ion} is estimated $-0.2\times10^{-4}\ \frac{emu}{mole}$. The Pauli paramagnetic term has thus about the same magnitude as χ_{VV}.

The third kind of experiments, applied to VO, are measurements of Seebeck coefficients. The Seebeck coefficient α of VO has been investigated by Banus *et al.* (8) and Aivazov *et al.* (16). Banus *et al.* found for α the value $-4\ \mu V/^{o}K$ at $300\ ^{o}K$, while Aivazov *et al.* conclude that α equals $10\ mV/^{o}K$. Banus' measurements show a linear dependence of α on T, which may indicate that the valence electrons are itinerant, while the negative value of α at room temperature is caused by the domination of the electrons over the holes in the conduction process (17). Due to experimental difficulties, useful Hall data are scarcely available until the present (10).

In this work we are trying to contribute to the discussion on the semiconductor-to-metal phenomenon. The most interesting compounds to investigate, are of course V_2O_3 and VO_2, which have resp. the corundum and the rutile structure. But their crystal structure has a rather low symmetry, while the primitive cells of V_2O_3 and VO_2 contain two molecules each, which complicates an ab-initio calculation. VO, with the cubic rocksalt structure and whose primitive cell contains one molecule, is easier to investi-

gate. We will therefore concentrate on this compound. On the basis of a band structure calculation we will try, in the way of Heine and Mattheiss (18) and Mattheiss (19), to elucidate the possible semiconductor-to-metal transition. In order to gain an insight into the influence of the temperature dependence, band structure calculations will be executed for several lattice constants. Special attention is given to the LCAO interpolation scheme for band energies, also used by Mattheiss (19). The results of the band structure calculations are thus translated into crystal-field parameters for V^{2+} in MgO. By extension of the basis functions to the 4s orbital of vanadium, we try to obtain a more realistic approximation of the fundamental interaction parameters.

The localized vs. collective electron model will be reviewed in chapter II. The semiconductor-to-metal transition models according to Mott, Falicov and Kimball, and Goodenough are also outlined in this chapter. The way in which some energy states of the energy band of VO are calculated by the APW method is outlined in chapter III. In chapter IV the LCAO interpolation method is presented, where its relation to crystal-field parameters is discussed. Chapter V gives the results of the combined APW-LCAO method. In our last chapter the results of this thesis are surveyed and evaluated.

* *The drawings of this thesis have been performed by Mr.A.J.Dekker.*

REFERENCES

1. MORIN F.J., *Phys. Rev. Letters* 3, 34 (1959)
2. MC WHAN D.B., MENTH A., REMEIKA J.P., BRINKMAN W.F. and RICE T.M., *Phys. Rev.* B 7, 1920 (1973)
3. KAWAKUBO T. and NAKAGAWA T., *J. Phys. Soc. Japan* 19, 517 (1964)
4. JAFFRAY J. and LYAND R., *J. des Recherches du C.N.R.S., Labs. Bellevue (Paris)* 4, 249 (1952)
5. AUSTIN I.G., *Phil. Mag.* 7, 961 (1962)
6. WARREN W.W., MIRANDA G.A. and CLARK W.G., *Bull. Am. Phys. Soc.* 12, 1117 (1967)
7. KAWANO S., KOSUGE K. and KACHI S., *J. Phys. Soc. Japan* 21, 2744 (1966)
8. BANUS M.D. and REED T.B., *Proc. Conf. on Chemistry of Extended Defects in Non-metallic Solids* (Edited by L.Eyring and

M.O'Keefe), p. 488, North Holland, Amsterdam (1970)
BANUS M.D., REED T.B. and STRAUSS A.J., *Phys. Rev.* B 5, 2775 (1972)
9. TAKEI H. and KOIDE S., *J. Phys. Soc. Japan* 24, 1394 (1968)
10. HONIG J.M., WAHNSIEDLER W.E., BANUS M.D. and REED T.B., *J. Solid State Chem.* 2, 74 (1970)
11. HONIG J.M. and WAHNSIEDLER W.E., *J. Phys. Chem. Solids* 33, 1836 (1972)
12. ANDERSON P.W., *Phys. Rev.* 109, 1492 (1958)
13. MASSARD P., BERNIER J.C. and MICHEL A., *Ann. Chim.* 4, 147 (1969)
14. SUZUKI K. and TAKEUCHI S., *Ferrites: Proc. of the Int. Conf.* (Edited by Y.Hoshino), p. 568, Univ. Park Press, Baltimore (1970)
15. AIVAZOV M.I., GUROV S.V. and SARKISYAN A.G., *Izv. Akad. Nauk. SSSR, Neorg. Mater.* 8, 213 (1972)
16. AIVAZOV M.I., DOMASHNEV A., SARKISYAN A.G. and GUROV S.V., *Izv. Akad. Nauk. SSSR, Neorg. Mater.* 8, 1069 (1972)
17. GOODENOUGH J.B., *Phys. Rev.* B 5, 2764 (1972)
18. HEINE V. and MATTHEISS L.F., *J. Phys. C* 4, L191 (1971)
19. MATTHEISS L.F., *Phys. Rev.* B 5, 290 (1972)

CHAPTER II - THE COLLECTIVE VERSUS LOCALIZED ELECTRON MODEL

2.1 INTRODUCTION

In 1932 Wilson (1) explained the fundamental difference between metals and non-metals. According to his theory the electrons of a solid are described by Bloch (2) orbitals:

$$\psi(\vec{k},\vec{r}) = \exp(i\vec{k}.\vec{r})w(\vec{k},\vec{r})$$

The corresponding energy eigenvalues form energy bands, which are a function of the wave vector $\vec{k}$. Wilson argues that in the case that an energy band is full and there is no overlap with other bands, the considered solid is an isolator. In the case of partially occupied bands, the solid is a metal.

However in 1937, de Boer *et al.* (3) suggested that Wilson's theory is not generally applicable to all solids. An example of such an exception is NiO. This substance has the rocksalt structure. We suppose that the cations are present as Ni^{2+} and the anions as O^{2-}. Ni^{2+} is in the state $(3d^8)$. The 3d functions in a cubic surrounding split in e_g and t_{2g} orbitals. According to band theory, the t_{2g} band shall be completely filled and the e_g band must be half full. Therefore NiO should be a conductor, however in practice it is an isolator.

De Boer *et al.* (3) assumed that the neglect of the Coulomb repulsion term U between two electrons on the same atom causes the contradiction between theory and experiment. For suppose that Ni^{2+} contains m valence electrons (m=8 in this case). We assume further that the term U is the *average* Coulomb repulsion energy of these valence electrons with opposite spin. The total repulsive energy will be Nm(m-1)U/2, where N is the number of nickel atoms in the crystal. The influence of the oxygen atoms is not considered here. If one electron from a certain Ni^{2+} goes to another cation, otherwise formulated, an Ni^{+} and an Ni^{3+} ion are created, the total repulsive energy becomes:

$$(N-2)m(m-1)U/2 + m(m+1)U/2 + (m-1)(m-2)U/2 =$$

$$Nm(m-1)U/2 + U$$

The conclusion is that the Coulomb repulsion term U will favor states, where all ions of the same kind have an equal number of electrons. In such a situation no metallic conductivity is feasible.

The ever returning question is how important the term U is for a given crystal. Depending on the magnitude of U, the electrons of a given crystal are best described by localized orbitals, Wannier functions (4), or itinerant orbitals, Bloch functions. In what case shall we apply crystal-field theory and when band theory? Apparently for NiO the Coulomb repulsion term is very important and NiO behaves as a semiconductor, where the residual conductivity is due to jumps of electrons between Ni^{2+} neighbours.

Stimulated by the observed sharp changes in the conductivity of vanadium oxides and related compounds, many theorists (5-15) have constructed models in order to explain the semiconductor-metal transition. We shall restrict ourselves here to three fundamental and essentially different descriptions.

In this chapter we present first the model of the transition according to Mott, which is more fundamentally formulated by Hubbard, further the model according to Falicov and Kimball, and in the last section Goodenough's model of the semiconductor-metal transition.

2.2 THE TRANSITION ACCORDING TO MOTT

Mott (5-7) has pointed out that the Coulomb repulsion term U plays an important role in the semiconductor-metal transition. In order to get some physical insight, we assume a three-dimensional crystal with hydrogen atoms, where only the 1s orbitals will be considered. We suppose the density of states, normalized to a number of states per atom, to be P(E) (see figure 2.1). Each state can contain two electrons viz. with α and β spin. Let n_+ and n_-

be the number of electrons with resp. α and β spin ($n = n_+ + n_-$), again normalized to a number per atom. In the case of non-interac-

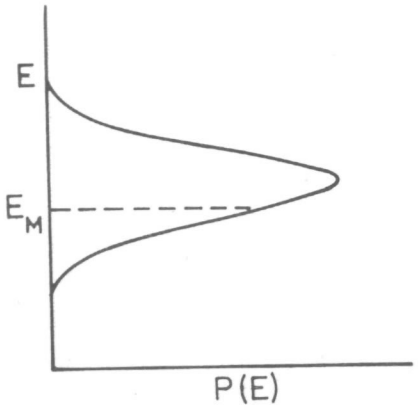

Fig. 2.1 The density of states P(E) of a model crystal.

tion, all states will be doubly filled up to a certain level and $n_+ = n_- = \frac{1}{2}n$. After introducing the Coulomb repulsion energy U between two electrons on an atom, the number of electrons with α and β spins may become unequal and the total energy E_t becomes approximately:

$$E_t = N\left[\int_{-\infty}^{E_+} EP(E)dE + \int_{-\infty}^{E_-} EP(E)dE + Un_+n_-\right]$$

E_+ and E_- refer to the maximum energy of the electrons with resp. α and β spin, while N is the number of atoms present. The interaction energy is the statical average over all possible distributions. We further know that:

$$n_+ = \int_{-\infty}^{E_+} P(E)dE$$

$$n_- = \int_{-\infty}^{E_-} P(E)dE$$

The equilibrium distribution at T=0 will be found by minimizing E_t vs. n_+ and investigating the stability of the solution obtained by the requirement $d^2E_t/dn_+^2 > 0$. In this way the following relations are obtained:

$$n_+ - n_- = (E_+ - E_-)/U \quad \ldots \{1\}$$

$$\frac{1}{P(E_+)} + \frac{1}{P(E_-)} > 2U \quad \ldots\ldots \{2\}$$

We can now distinguish two cases: 1^0 stable solution $n_+ = n_-$
2^0 stable solutions $n_+ >> n_-$

Since for the first solution $E_+ = E_- = E_M$ (see figure 2.1), this leads to the requirement:

$$P(E_M) < 1/U$$

$P(E_M)$ is approximately inversely proportional to the bandwidth W. Therefore in this situation $W > cU$, where c is a constant.

In the case that

$$P(E_M) > 1/U \qquad (W < cU)$$

$n_+ \neq n_-$ and there will be more electrons with α than β spin. Depending on the total number of electrons n and the shape of P(E), either the most extreme case will be realized, where $n_+ = n$ and $n_- = 0$, or an intermediate stable solution exists (see further figure 2.2).

In the description as given above, the solution $n_+ = n_-$

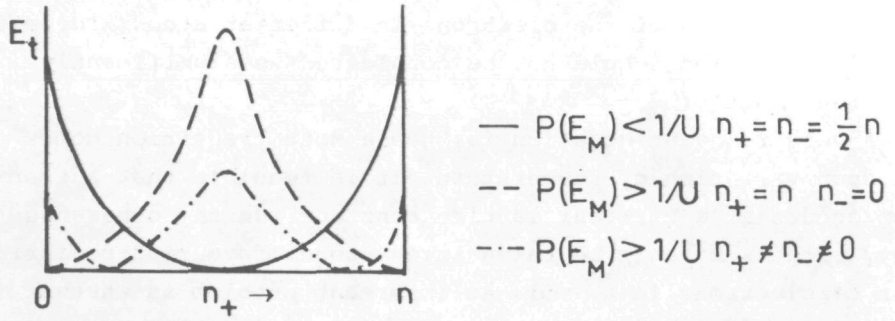

Fig. 2.2 The total energy E_t as a function of n_+ for several possible cases.

represents the metallic conductor with uncorrelated electrons, the solution $n_+ >> n_-$ the isolator with strongly correlated electrons.

Hubbard (8-10) has formulated the problem more exactly by a model Hamiltonian, which is known to be the Hubbard Hamiltonian:

$$H_h = \sum_{i,j} \sum_{\sigma} T_{ij} c^{\dagger}_{i\sigma} c_{j\sigma} + \tfrac{1}{2} U \sum_{i,\sigma} n_{i\sigma} n_{i,-\sigma} \quad .... \{3\}$$

where $c^{\dagger}_{i\sigma}$ and $c_{i\sigma}$ are the creation and destruction operators for electrons with spin σ in the Wannier (4) state centered on site $\vec{t}_i$. We note that a Wannier function is an orthonormalized atomic orbital. T_{ij} is the Fourier transform of the Bloch energies $E(\vec{k})$ and $n_{i\sigma}$ is the operator related to the number of electrons on site $\vec{t}_i$. This model Hamiltonian has been formulated, for reasons of mathematical simplicity, for the case of a crystal only containing s electrons. The calculation of the eigenvalues of the Hubbard Hamiltonian is executed formally, that is with the help of a Green's function technique. Hubbard concludes that if $W < \frac{2}{3}\sqrt{3}(U)$ the energy band with a bandwidth W splits in two narrow subbands and the free electron band theory has to be replaced by a strong correlation model.

Mott (5-7), who was the first who explained this semiconductor-metal transition mechanism, has found the criterium $U > W$ for bandsplitting. Hubbard has conjectured that the results of his theory should be treated with some caution because of the neglect of the interactions of the electrons on different atoms. Therefore Hubbard's criterium should not be considered as significantly better than Mott's.

A very relevant question is, how a Mott transition comes about upon variation of temperature. It is feasible that a transition occurs at a critical lattice constant. On the other hand entropy effects have to be taken into account favouring redistribution of electrons in a band. An important problem is whether the transition is a gradual process or it arrives sharply at a critical temperature as a consequence of a cooperative phenomenon. Mott (7) argues in favor of the latter proposition. His arguments

are based on the fact that if we have created a free moving hole and electron, these two "particles" would attract each other via a Coulomb interaction, $V(r) = -e^2/\kappa r$ and form a so-called "exciton", where κ is the dielectric constant. The formation of the exciton prevents the electron and hole to participate in the conduction process. However, if more electrons and holes are present, an electron and a hole will attract each other via a screened Coulomb interaction, $V(r) = (-e^2/\kappa r)\exp(-\alpha r)$, where α is the screening constant. If there is a sufficient number of carriers, α becomes so large that the excitons disintegrate and a sharp transition from no free carriers to a large number occurs. It shall be clear that the repulsion term U becomes also smaller because of the screening effect.

Finally, we like to pay attention to the magnetic properties of a solid near the Mott transition. Making use of Hubbard's Hamiltonian, Brinkman and Rice (11) have considered a solid, which is just on the metallic side of the Mott transition. The solid consists of atoms containing only one electron each. They find a highly correlated electron gas, which is nonmagnetic. Besides, there is an enhancement of the effective mass and the Pauli paramagnetism.

2.3 THE TRANSITION ACCORDING TO FALICOV AND KIMBALL (12)

This model is based on the simultaneous existence of localized and collective states, where the localized states are situated just underneath the conduction band. At T = 0 the localized states are assumed to be fully occupied by electrons, while the higher collective states are empty. As the temperature T rises, electrons will be excited to the collective states. That is, a localized hole and an itinerant electron are created. Further assuming that it is impossible that more than one electron per atom is excited, the most important terms of the model Hamiltonian, in the spirit of Hubbard, will be:

$$H_o = \sum_{\nu,\vec{k},\sigma} E_\nu(\vec{k}) a^\dagger_{\nu\vec{k}\sigma} a_{\nu\vec{k}\sigma} + \sum_{i,\sigma} \varepsilon b^\dagger_{i\sigma} b_{i\sigma}$$

$$+ \sum_{i,\sigma,\sigma',\nu,\nu'} G b^\dagger_{i\sigma} c^\dagger_{\nu i\sigma'} c_{\nu' i\sigma'} b_{i\sigma}$$

where $a^\dagger_{\nu\vec{k}\sigma}$ creates an electron in state $\vec{k}$, band ν, with spin σ, $b^\dagger_{i\sigma}$ creates a hole with spin σ at site $\vec{t}_i$ and $c^\dagger_{\nu i\sigma}$ creates the Wannier states corresponding to the Bloch bands $\nu\sigma$. The first two sums are the one-particle terms, the last sum represents the intra-atomic interaction between a localized hole and a delocalized electron. The essentials of this description are found in the following expression for the free energy F of the system:

$$F = N\{\Delta n - Gn^2 + \text{entropy terms}\}$$

where N is the number of atoms, n the number of electrons in the conduction band (equal to the number of localized holes) and Δ the energy gap for the formation of an electron-hole pair. n is normalized to a number of states per atom. We have in fact an effective energy gap $\Delta_{eff} = \Delta - 2Gn$, which decreases as n increases. The thermodynamic requirement that F must be minimum as a function of n, gives us the dependence of n on the temperature T. The theory is further similar to the Bragg-Williams treatment of phase transitions. For certain values of G, the n vs. T curves show a discontinuity. This implicates at the same time a discontinuity in the conductivity vs. T curves, which indicates a semiconductor-metal transition.

It is seen that the Falicov-Kimball treatment is not restricted to T = 0 and that the entropy terms are essential in causing the transition.

2.4 THE SEMICONDUCTOR-METAL TRANSITION ACCORDING TO GOODENOUGH

The essential feature of Goodenough's theory (13,14) is a change in symmetry at a certain temperature (first order phase

transition), leading to a change in band structure. Generally at higher temperatures a more symmetric structure will be found, while at lower temperatures the structure is less symmetric. Completely similar to crystal-field splittings of the electronic energy levels of isolated atoms, which is the leading principle of Goodenough, higher symmetry will lead to higher degeneracies in the band structure than lower symmetries. Thus it is feasible that a band, partially filled at high temperatures (for instance a t_{2g} band of V^{4+}), splits up into a completely filled band and a completely empty band below the transition temperature. If the two latter bands are well separated, the metallic conductor of the high temperatures is transformed into an isolator by decreasing the temperature through the transition point.

Two mechanisms might be considered as responsible for the preference of rather low symmetries at low temperatures:

1° Jahn-Teller effects, where an orbital degenerate symmetric state gains in energy by removal of the degeneracy.

2° Metal-metal bonding effects, where spin correlation of unpaired spins on neighbouring pairs of metal atoms may distort a linear chain of equidistant atoms into pairs of bound atoms with alternating short and long separations.

At high temperatures entropy effects will prevail generally and the more symmetric structures will dominate in the same way as is found for transitions between static and dynamic Jahn-Teller effects.

REFERENCES

1. WILSON A.H., *Proc. R. Soc.* 133, 458 (1931)
2. BLOCH F., *Z. Physik* 52, 555 (1928)
3. DE BOER J.H. and VERWEY E.J.W., *Proc. Phys. Soc. (London)* 49, 59 (1937)
4. WANNIER G.H., *Phys. Rev.* 52, 191 (1937)
5. MOTT N.F., *Proc. Phys. Soc. (London)* A 62, 416 (1949)
6. MOTT N.F., *Phil. Mag.* 24, 935 (1971)
7. MOTT N.F., *Contemp. Phys.* 14, 401 (1973)
8. HUBBARD J., *Proc. Roy. Soc.* A 276, 238 (1963)
9. HUBBARD J., *Proc. Roy. Soc.* A 277, 237 (1964a)
10. HUBBARD J., *Proc. Roy. Soc.* A 281, 401 (1964b)

11. BRINKMAN W.F. and RICE T.M., *Phys. Rev.* B 2, 4302 (1970)
12. FALICOV L.M. and KIMBALL J.C., *Phys. Rev. Letters* 22, 997 (1969)
13. GOODENOUGH J.B., *Czech. J. Phys.* B 17, 304 (1967)
14. GOODENOUGH J.B., in *Progress in Inorganic Chemistry* (Edited by H.Reiss), Vol. 5, p. 145, Pergamon Press, New York (1971)
15. ADLER D., *Rev. Mod. Phys.* 40, 714 (1968b)

CHAPTER III - BAND STRUCTURE CALCULATIONS

- APW METHOD -

3.1 INTRODUCTION

A band structure calculation is usually executed in order to get information about the physical properties of the concerning crystal. Interesting quantities are e.g. the Fermi energy E_F and the density of states P(E) (these two quantities are important in relation to the degree of occupation of the valence bands and the bandwidth, which determine whether the considered solid is an insulator or a conductor). For this purpose we need the eigenvalues $E(\vec{k})$ in a great number (10^4-10^5) of $\vec{k}$-points in the Brillouin zone. It is well-known that an ab-initio calculation like the APW method is a costly procedure, for it consumes rather much computer time. Consequently it is impossible to obtain sufficient information from an ab-initio calculation. So the ab-initio calculation is normally restricted to a few symmetry points in the Brillouin zone. The other eigenvalues $E(\vec{k})$ are then obtained by an interpolation method that will be described in the next chapter.

3.2 THE BORN - VON KARMAN BOUNDARY CONDITION

The boundary condition plays a very important role in quantum mechanics, for the Schrödinger equation is a second order differential equation with solutions strongly dependent on boundary conditions. Finite dimensions of a solid leads to mathematical difficulties at the edge of the crystal. It is therefore advantageous to suppose the crystal infinitely large. The one-electron Schrödinger equation for such a problem is:

$$\{-\vec{\nabla}^2 + V(\vec{r})\}\psi(\vec{r}) = E\psi(\vec{r})$$

where E is the one-electron eigenvalue and $V(\vec{r})$ is the potential. In the crystal there is a translational symmetry represented by

the translation vectors $\vec{t}_n$. The potential will be a repeating quantity, mathematically denoted by:

$$V(\vec{r}+\vec{t}_n) = V(\vec{r})$$

Although it is now possible to solve the one-electron Schrödinger equation, since the crystal extends indefinitely in each direction, there is a continuum of solutions. This also causes mathematical problems, since we can only deal with finite numbers. To avoid these complications, so-called periodic boundary conditions are invoked in an otherwise infinite crystal. For the x-, y- and z-direction we conjecture respectively N_1, N_2 and N_3 repeating units and require all wave functions to have a three-dimensional periodicity according to the "supercell" consisting of $N_1N_2N_3$ unit cells. Mathematically formulated we will have:

$$\psi(\vec{r}) = \psi(\vec{r}+N_1\vec{a}_1) = \psi(\vec{r}+N_2\vec{a}_2) = \psi(\vec{r}+N_3\vec{a}_3)$$

$\vec{a}_1$, $\vec{a}_2$ and $\vec{a}_3$ are the primitive translation vectors in respectively the x-, y- and z-direction. It is evident that N_1, N_2 and N_3 should not be too small in order to get significant results. The outlined boundary condition is often referred to as the Born cyclic boundary condition. It was proposed by Born and von Kármán (1).

3.3 BLOCH'S THEOREM

The shape of the wave functions in a crystal is governed by its translational symmetry. Let us introduce the translation operators $\vec{t}_n$, defined in such a way that these operators, operating on the coordinates $\vec{r}$, transform them in $\vec{r}-\vec{t}_n$. Translation symmetry means that the potential $V(\vec{r})$ is invariant under all translation operators $\vec{t}_n$, where the related translation vectors $\vec{t}_n$ ($\vec{t}_n = n_1\vec{a}_1 + n_2\vec{a}_2 + n_3\vec{a}_3$) belong to the points of a three-dimensional lattice. This is also true for the kinetic part of the Hamiltonian. Consequently the complete Hamilton operator

does not change if a translation operator of the lattice is applied to it:

$$\vec{t}_n H(\vec{r}) = H(\vec{r})$$

For that reason the translation and the Hamilton operator commute with each other when they operate on a wave function. But this means that they have a simultaneous set eigenfunctions $\psi(\vec{r})$.

The eigenfunctions of the translation operators are found by the application of the projection operator formalism. Let us define the primitive vectors of the reciprocal lattice $\vec{b}_1$, $\vec{b}_2$ and $\vec{b}_3$ by the relation $\vec{a}_i.\vec{b}_j = \delta_{ij}$. The values of the wave vectors $\vec{k}$ consistent with the Born-von Kármán boundary conditions then have the form:

$$\vec{k} = 2\pi(k_1\vec{b}_1 + k_2\vec{b}_2 + k_3\vec{b}_3);$$

$$(k_i = p_i/N_i;\ 0 < p_i \leqq N_i;\ i = 1, 2, 3)$$

As the translation group is Abelian, all representations are one-dimensional. The characters of these representations are given by $\exp(i\vec{k}.\vec{t}_n)$, where $\vec{k}$ specifies the irreducible representations of the translation group and is limited to the values given above. The projection operator associated with the $\vec{k}$-th irreducible representation of the translation group thus is (2):

$$O(\vec{k}) = (1/O_t) \sum_n \exp(-i\vec{k}.\vec{t}_n)\vec{t}_n$$

where O_t denotes the order of the translation group. The sum includes all translations of the crystal. Application of $O(\vec{k})$ on an arbitrary wave function $F(\vec{r})$ results in a so-called Bloch function:

$$O(\vec{k})F(\vec{r}) = (1/O_t) \sum_n \exp(-i\vec{k}.\vec{t}_n)F(\vec{r}-\vec{t}_n)$$

$$= \exp(-i\vec{k}.\vec{r})w(\vec{k},\vec{r}) \quad \ldots \{1\}$$

where

$$w(\vec{k},\vec{r}) = \{(1/O_t) \sum_n \exp(i\vec{k}.(\vec{r}-\vec{t}_n))F(\vec{r}-\vec{t}_n)\}$$

It is easy to verify that an arbitrary translation operator $\vec{t}_n$ leaves $w(\vec{k},\vec{r})$ invariant:

$$\vec{t}_n w(\vec{k},\vec{r}) = w(\vec{k},\vec{r})$$

moreover

$$\vec{t}_n\{O(\vec{k})F(\vec{r})\} = \exp(i\vec{k}.\vec{t}_n)\{O(\vec{k})F(\vec{r})\} \quad \ldots \{2\}$$

These projected wave functions $\psi(\vec{k},\vec{r})$ $\{=O(\vec{k})F(\vec{r})\}$ or Bloch functions have the right symmetry for the Schrödinger equation of our periodical potential problem:

$$H\psi(\vec{k},\vec{r}) = E(\vec{k})\psi(\vec{k},\vec{r})$$

3.4 THE BRILLOUIN ZONES

The vectors $\vec{b}_1$, $\vec{b}_2$ and $\vec{b}_3$ have been defined in the preceding part. In terms of these vectors of the reciprocal lattice we set up vectors $\vec{K}_m$ that satisfy the relation:

$$\vec{K}_m = 2\pi(h_1\vec{b}_1 + h_2\vec{b}_2 + h_3\vec{b}_3)$$

where h_1, h_2 and h_3 are integers. These vectors $\vec{K}_m$ form the translation vectors of the reciprocal lattice, which is constructed by the basis vectors $\vec{b}_1$, $\vec{b}_2$ and $\vec{b}_3$. They have the property that:

$$\exp(i\vec{K}_m.\vec{t}_n) = 1 \quad \ldots \{3\}$$

If we now consider equation (2) we ascertain that $\vec{k}$ is not unambiguously defined. For take $\vec{k}' = \vec{k} + \vec{K}_m$ and calling in mind equation (3), relation (2) changes then in:

$$\vec{t}_n\psi(\vec{k},\vec{r}) = \exp(i\vec{k}'.\vec{t}_n)\exp(-i\vec{K}_m.\vec{t}_n)\psi(\vec{k},\vec{r})$$

$$= \exp(i\vec{k}'.\vec{t}_n)\psi(\vec{k},\vec{r})$$

The conclusion is that $\vec{k}$ and $\vec{k}'$ represent the same representation of the translation group. For that reason we define $\vec{k}$-space consisting of those points that lie closer to $\vec{k} = (0,0,0)$ than to any other reciprocal lattice point. We call this the *first* Brillouin zone. Its boundaries are formed by the perpendicular bisector planes of the lines that connect the nearer reciprocal points with the origin $\vec{k} = (0,0,0)$.

3.5 ROTATIONAL SYMMETRY IN THE SOLID STATE

Besides translation operations there are rotation operations R possible in the solid state. All the combinations of rotations and translations symbolized by $\{R|\vec{t}_n\}$ form a group, which is called a symmorphic space group. We do not consider the combinations of e.g. a rotation and a non-primitive translation. these latter groups are so-called non-symmorphic space groups. A rigorous and formal description of space groups is rather complicated. For the interested reader we refer to Jansen *et al.* (2).

After introduction of rotational symmetry, the space group of a crystal is no longer Abelian. The irreducible representations may therefore have higher orders than one. The dimensions of the irreducible representations depend on the position in $\vec{k}$-space. Consequently the degeneracy of the energy levels depends on $\vec{k}$. For the underlying ideas we restrict ourselves to the following intuitive description.

Suppose we let operate the rotation operator R on a Bloch function $\psi(\vec{k},\vec{r})$, where

$$\psi(\vec{k},\vec{r}) = \exp(-i\vec{k}.\vec{r})w(\vec{k},\vec{r})$$

This will result in:

$$R\psi(\vec{k},\vec{r}) = \exp(-i\vec{k}.R^{-1}\vec{r})w(\vec{k},R^{-1}\vec{r})$$

Applying the same rotation operator to both vectors of a scalar product does not change its value, therefore:

$$\vec{k}.R^{-1}\vec{r} = R\vec{k}.RR^{-1}\vec{r} = R\vec{k}.\vec{r}$$

Using this result, we have:

$$R\psi(\vec{k},\vec{r}) = \exp(-iR\vec{k}.\vec{r})w(\vec{k},R^{-1}\vec{r})$$

The rotation $\{R|0\}$ belongs to the space group, hence

$$R^{-1}(\vec{r}+\vec{t}_n) = R^{-1}\vec{r} + \vec{t}_m$$

Thus the function $w(\vec{k},R^{-1}\vec{r})$ is a periodic function because $w(\vec{k},\vec{r})$ is periodic. We rename the function $w(\vec{k},R^{-1}\vec{r})$ in $w'(R\vec{k},\vec{r})$. We have now:

$$R\psi(\vec{k},\vec{r}) = \exp(-iR\vec{k}.\vec{r})w'(R\vec{k},\vec{r})$$

The conclusion is that operating on a Bloch function with a rotation operator produces another Bloch function with the $\vec{k}$-vector simply rotated to $R\vec{k}$.

It seems now plausible that those symmetry operations that transform a wave function, characterized by a vector $\vec{k}$, to a new wave function, characterized by the same wave vector $\vec{k}$, play an important role. The rotation operators R, which in this sense fulfill the relation $R\vec{k} = \vec{k} + \vec{K}_m$, where $\vec{K}_m$ is an arbitrary reciprocal lattice vector, form a subgroup of the entire point group of the crystal. This subgroup is called the *group of the wave vector*, while it is also known as the *small* or *little group* of $\vec{k}$. Now, under an operation of the group of $\vec{k}$, $\psi(\vec{k},\vec{r})$ may be left unchanged or will be transformed into a new function $\psi'(\vec{k},\vec{r})$ with the same wave vector $\vec{k}$. In this latter case, there

is more than one distinct $w(\vec{k},\vec{r})$ associated with the same exponential factor $\exp(i\vec{k}.\vec{r})$. These various $w(\vec{k},\vec{r})$ transform into each other according to an irreducible representation of the group of the wave vector $\vec{k}$.

We summarize that the wave functions of a solid ought to be classified according to their wave vectors $\vec{k}$. Wave functions with the same wave vector are further classified according to the irreducible representations of the little group of the wave vector $\vec{k}$. The preceding considerations are illustrated by figure 3.1, where the first Brillouin zone of fcc VO is shown, the Greek

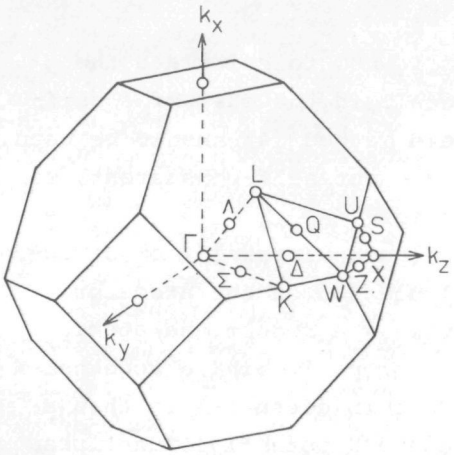

Fig. 3.1 The first Brillouin zone of fcc VO.

letters symbolize the little group of $\vec{k}$. We establish that there are symmetry lines viz. Σ, Δ, Q, S and Z whose corresponding little groups are the resp. point groups C_{2h}, C_{4v}, C_2, C_{2h} and C_{2h}, and symmetry points viz. Γ, K, L, U, X and W whose corresponding little groups are the resp. point groups O_h, C_{2h}, D_{3d}, C_{2h}, D_{4h} and C_{4v}. There are also symmetry planes present e.g. the plane ΓKL, however from the calculational point of view they are of less importance.

3.6 THE MUFFIN-TIN POTENTIAL †

The Augmented Plane-Wave (APW) method, which has been set up by Slater (3) in 1937 for calculating the energy band structure of solids, makes use of a model potential. The basic idea is the subdivision of the solid into two types of regions. Around each atom a sphere of radius R_n is constructed in such a way that different spheres can't overlap each other. Within the spheres the crystal potential is assumed spherically symmetric, while in the outside region the potential is supposed to be constant. This model potential is often called the *muffin-tin* potential.

The first question that arises is how to calculate the muffin-tin potential in a given crystal. In the case of a self-consistent field calculation the Ewald method (4) has to be used. Since in this work the calculations are not self-consistent, we focus our attention on this latter case.

The starting point is a Hartree-Fock-Slater (5) or Dirac-Slater (6) self-consistent field calculation of the atoms or ions composing the lattice. This gives as a result the atomic charge density and Coulomb potential, properly linked together by Poisson's equation. The crystal Coulomb potential is then a superposition of these free atomic Coulomb potential functions, centered on the different sites of the crystal.

Inside the muffin-tin spheres, the potential is assumed spherically symmetric. The spherically averaged Coulomb potential can easily be calculated by the so-called α-Löwdin (7) expansion. Supposing that the atomic Coulomb potential of the i'th atom is $U_i(r)$, the spherically averaged superposed Coulomb potential within the i'th muffin-tin sphere is:

$$V_i(r) = U_i(r) + \sum_{j \neq i} \frac{1}{2rr_j} \int_{|r_j - r|}^{r_j + r} \xi U_j(\xi) d\xi$$

† *The muffin-tin potential is calculated by the program* MTPOT, *which has been developed in the course of this work (see further Appendix II).*

$U_j(r)$ is the atomic Coulomb potential of a neighbouring atom j somewhere in the lattice at a distance r_j. In order to obtain reasonable approximations of the self-consistent wave functions of the crystal side by side with the Coulomb potential, the exchange potential has to be inserted in the Schrödinger equation. This inclusion of the exchange potential is a crucial point. The approximation accepted for these purposes is the one electron Slater exchange approximation (8,9):

$$V_{exch}(r) = -6\alpha\left(\frac{3}{8\pi}\,\rho(r)\right)^{1/3} \qquad \left(\frac{2}{3} \leq \alpha \leq 1\right)$$

where the exchange potential is directly related to the electronic charge density $\rho(r)$. α is a constant, $\alpha=1$ is called Slater full exchange. The required electronic charge density of the crystal in its turn is obtained by superposition of the atomic charge densities, where again spherical symmetry inside the muffin-tin spheres is obtained by an averaging procedure.

The Coulomb potential in the regions between the muffin-tin spheres is averaged out according to the integral method of Ham and Segall (10). They have derived in their paper the relation:

$$\{\Omega - \sum_i \tfrac{4}{3}\pi R_i^3\}V_c = 4\pi \sum_i \int_0^{\infty} r^2 U_i(r)\,dr - 4\pi \sum_i \int_0^{R_i} r^2 V_i(r)\,dr$$

where V_c is the constant Coulomb potential, Ω is the volume of the unit cell and R_i is the muffin-tin sphere of the i'th atom in the cell. The summation Σ_i is executed over the atoms of the unit cell.

The exchange potential in the regions between the muffin-tin spheres, calculated according to the Slater approximation, again requires the charge density. Once knowing the electronic charge density distribution inside the muffin-tin spheres, because of the charge neutrality in the entire unit cell, the mean electron charge in the outside region can be derived. If this mean charge density is $\bar{\rho}$, the resulting exchange potential

is put constant and equal to:

$$-6\alpha\left(\frac{3}{8\pi}\,\bar{\rho}\right)^{1/3}$$

3.7 THE APW FORMALISM APPLIED TO THE MUFFIN-TIN POTENTIAL *

The problem to solve is the one-electron Schrödinger equation for a periodic solid:

$$H\psi(\vec{k},\vec{r}) \equiv \{-\vec{\nabla}^2 + V(\vec{r})\}\psi(\vec{k},\vec{r}) = E(\vec{k})\psi(\vec{k},\vec{r})$$

The physical quantities are expressed in atomic units (au), while the Rydberg (Ry) is taken as energy unit. The one-electron potential $V(\vec{r})$ is the muffin-tin potential, which is the sum of the Coulomb and exchange potential. For simplicity we assume that the constant potential outside the muffin-tin spheres is shifted to zero. The potential $V(\vec{r})$ is a periodic function, invariant under a translation operation of the lattice:

$$V(\vec{r}+\vec{t}_n) = V(\vec{r})$$

$\vec{t}_n$ is an appropriate lattice vector of the crystal. According to paragraph 3.3 the wave functions are Bloch type functions:

$$\psi(\vec{k},\vec{r}) = \exp(i\vec{k}.\vec{r})w(\vec{k},\vec{r})$$

where $w(\vec{k},\vec{r})$ is a periodic function:

$$w(\vec{k},\vec{r}+\vec{t}_n) = w(\vec{k},\vec{r})$$

The function $\psi(\vec{k},\vec{r})$ cannot be calculated directly as a solution of the mentioned Schrödinger equation. Therefore $\psi(\vec{k},\vec{r})$ is expanded in terms of the so-called APW functions:

* *The program* (S)APW *that handles the symmetry adapted APW method, was supplied by Dr.D.A.Papaconstantopoulos.*

$$\psi(\vec{k},\vec{r}) = \sum_i c(\vec{k}_i)\phi(\vec{k}_i,\vec{r};E)$$

The wave functions $\phi(\vec{k}_i,\vec{r};E)$ represent a plane wave with wave vector $\vec{k}_i$ in the region outside the muffin-tin spheres:

$$\phi(\vec{k}_i,\vec{r};E) = \exp(i\vec{k}_i.\vec{r})$$

where $\vec{k}_i = \vec{k} + \vec{K}_i$, while $\vec{K}_i$ is a translation vector of the reciprocal lattice. Within the muffin-tin spheres, the ϕ's are expanded in terms of products of spherical harmonics and radial wave functions. Inside an APW sphere, centered on the atom located at $\vec{r}_n$, we have (for $\vec{r}-\vec{r}_n$ the variable $\vec{r}'$ is substituted):

$$\phi(\vec{k}_i,\vec{r};E) = \sum_{l=0}^{\infty} \sum_{m=-l}^{+l} A_{lm}(\vec{k}_i)u_l(|\vec{r}'|;E)Y_{lm}(r')$$

where $A_{lm}(\vec{k}_i)$ are constants, r' indicates the angular part of $\vec{r}'$. The functions $u_l(|\vec{r}'|;E)$ are solutions of the radial Schrödinger equation:

$$-\frac{1}{r'^2}\frac{d}{dr'}\left[r'^2\frac{du_l}{dr'}\right] + \left[\frac{l(l+1)}{r'^2} + V(r')\right]u_l = Eu_l$$

We are still at liberty to choose the constants $A_{lm}(\vec{k}_i)$. In the APW formalism the ϕ's are assumed to be continuous functions. So at the muffin-tin spheres the plane wave has to fit to the spherically harmonic expansion. It is well-known in literature that a plane wave can be expanded in terms of products of spherical harmonics and spherical Bessel functions. In the case the expansion is executed around the centre $\vec{r}_n$, we have:

$$e^{i\vec{k}_i.\vec{r}} = e^{i\vec{k}_i.(\vec{r}'+\vec{r}_n)}$$

$$= 4\pi e^{i\vec{k}_i.\vec{r}_n} \sum_{l=0}^{\infty} \sum_{m=-l}^{+l} i^l J_l(k_i r')Y^*_{lm}(k_i)Y_{lm}(r')$$

where $J_l(x)$ is a spherical Bessel function of order l and k_i is the angular part of $\vec{k}_i$. Consequently at the sphere radius R_n the following relation holds:

$$A_{lm}(\vec{k}_i) = 4\pi e^{i\vec{k}_i\cdot\vec{r}_n}\, i^l Y^*_{lm}(k_i) J_l(k_i R_n)/u_l(R_n;E)$$

Therefore the APW function for the state specified by the wave vector $\vec{k}_i$ is:

$$e^{i\vec{k}_i\cdot\vec{r}} \qquad \text{(outside spheres)}$$

$$4\pi e^{i\vec{k}_i\cdot\vec{r}_n} \sum_{l=0}^{\infty} \sum_{m=-l}^{+l} i^l J_l(k_i R_n) Y^*_{lm}(k_i) Y_{lm}(r') \times$$

$$u_l(r';E)/u_l(R_n;E) \qquad \text{(inside the n'th sphere)}$$

This APW function is obviously no good quantum mechanical wave function because of the discontinuity of its derivative at the muffin-tin spheres.

We consider now our original function $\psi(\vec{k},\vec{r})$, which is an expansion of APW functions. In order to know the expansion coefficients $c(\vec{k}_i)$, related to the wave function $\psi(\vec{k},\vec{r})$, and additionally the minimum energy, the variational method is used. To this end the matrix elements of H-E between the APW's have to be calculated. Consider:

$$(H-E)_{ij} = \int^{cell} \phi(\vec{k}_i,\vec{r};E)^* (H-E)\phi(\vec{k}_j,\vec{r};E)\,dv$$

$$= \int^{cell} \{\vec{\nabla}\phi(\vec{k}_i,\vec{r};E)^*.\vec{\nabla}\phi(\vec{k}_j,\vec{r};E) +$$

$$(V-E)\phi(\vec{k}_i,\vec{r};E)^*\phi(\vec{k}_j,\vec{r};E)\}dv$$

This integration can be carried out straightforwardly. The discontinuity in the functions $\nabla\phi(\vec{k}_i,\vec{r};E)$ at the muffin-tin spheres is accounted for by applying Green's theorem in the form:

$$\int^{cell} \vec{\nabla} f.\vec{\nabla} g \; dv = \int_S f\vec{\nabla} g.d\vec{S} - \int^{cell} f\vec{\nabla}^2 g \; dv$$

f and g are APW functions, S denotes the surface where the slopes

of the APW functions are discontinuous. The result of the integration is:

$$\Omega^{-1}(H-E)_{ij} = (\vec{k}_i.\vec{k}_j-E)\delta_{ij} + \sum_n \exp\{i(\vec{k}_j-\vec{k}_i).\vec{r}_n\}F_{ijn} \quad \ldots \{4\}$$

where

$$F_{ijn} = \{4\pi R_n^2/\Omega\}\Big[-(\vec{k}_i.\vec{k}_j-E)J_1(|\vec{k}_j-\vec{k}_i|R_n)/|\vec{k}_j-\vec{k}_i| + \sum_{l=0}^{\infty}(2l+1)P_l(\vec{k}_i.\vec{k}_j)J_l(k_iR_n)J_l(k_jR_n)\times \{u_l'(R_n;E)/u_l(R_n;E)\}\Big] \quad \ldots \{5\}$$

Ω is the volume of the unit cell, $P_l(x)$ and $J_l(x)$ represent the Legendre polynomials and spherical Bessel functions, while $\vec{k}_i$ equals $\vec{k}_i/k_i$.

Knowing the matrix elements, the eigenvalues and eigenvectors follow from the secular equation:

$$\| H - SE \| = 0 \qquad (S \text{ is the overlap matrix})$$

Because of the way the problem has been set up, the matrix elements H_{ij} are a function of the energy E. So the secular equation has to be solved by a trial and error method instead of a direct diagonalisation. We evaluate therefore the matrix elements and the secular determinant as a function of energy and use an interpolation scheme to determine the zeros.

Since the above mentioned calculation consumes rather much computer time, it is advantageous to use symmetry adapted APW's that reduce the size of the secular determinant. The projection operator for Bloch functions is:

$$\rho^{\alpha}_{ij} = \sum_R \{\Gamma^{\alpha}_{ij}(R)\}^{*}R$$

where the summation is over all the elements of the so-called little group $G_{\vec{k}}$ of the wave vector $\vec{k}$. This group is an assembly

of all space group operations, whose rotational parts R satisfy the relation:

$$R\vec{k} = \vec{k} + \vec{K}_i$$

$\Gamma^{\alpha}_{ij}(R)$ is the ij'th element of the α'th representation, representing the operator R.

We are now interested in knowing the matrix elements of the projected functions $\phi(\vec{k}_i,\vec{r};E)$ and $\phi(\vec{k}_j,\vec{r};E)$. The orthogonality properties of the projection operators tell us, that:

$$\langle\rho^{\alpha}_{ij}F_1|H|\rho^{\beta}_{kl}F_2\rangle = (g/n_{\alpha})\langle F_1|H|\rho^{\alpha}_{jl}F_2\rangle\delta_{\alpha\beta}\delta_{ik}$$

g is the order of the group $G_{\vec{k}}$, n_{α} is the dimension of the α'th representation. Thus we may restrict ourselves from the beginning to consider one representation at a time. Hence:

$$\begin{aligned}(H-E)_{ij} &= \langle\rho^{\alpha}_{11}\phi(\vec{k}_i,\vec{r};E)\,|H-E|\,\rho^{\alpha}_{11}\phi(\vec{k}_j,\vec{r};E)\rangle \\ &= (g/n_{\alpha})\langle\phi(\vec{k}_i,\vec{r};E)\,|H-E|\,\rho^{\alpha}_{11}\phi(\vec{k}_j,\vec{r};E)\rangle \\ &= (g/n_{\alpha})\sum_R \{\Gamma^{\alpha}_{11}(R)\}^{*}\langle\phi(\vec{k}_i,\vec{r};E)\,|H-E|\,\phi(R\vec{k}_j,\vec{r};E)\rangle\end{aligned}$$

Continuing straightforwardly, gives us the symmetrized equivalent of the earlier mentioned secular equation. The matrix elements are:

$$\begin{aligned}\Omega^{-1}(H-E)_{ij} = (g/n_{\alpha})\sum_R \{\Gamma^{\alpha}_{11}(R)\}^{*}\Big[&(\vec{k}_i.R\vec{k}_j-E)\,\delta(R\vec{k}_j,\vec{k}_i) \\ &+ \sum_n \exp\{i(R\vec{k}_j-\vec{k}_i).\vec{r}_n\}F_{ijn}(R)\Big]\end{aligned}$$

where

$$\begin{aligned}F_{ijn}(R) = \{4\pi R_n^2/\Omega\}\Big[&-(\vec{k}_i.R\vec{k}_j)J_1(|R\vec{k}_j-\vec{k}_i|R_n)/|R\vec{k}_j-\vec{k}_i| \\ &+ \sum_{l=0}^{\infty}(2l+1)P_l(\vec{k}_i.R\vec{k}_j)J_l(k_iR_n)J_l(k_jR_n)\Big[\frac{u_l'(R_n;E)}{u_l(R_n;E)}\Big]\Big]\end{aligned}$$

3.8 THE EXTENSION OF THE APW METHOD †

In the preceding pages we defined the muffin-tin potential as being spherically symmetric inside the APW spheres and constant outside. It will also be convenient to express a potential as a muffin-tin part plus a remainder. The smallness of the remainder will be a measure for the validity of the APW method as mentioned above.

Suppose that our one-electron Hamiltonian, expressed in atomic units, is:

$$H = -\vec{\nabla}^2 + V_m(\vec{r}) + V_1(\vec{r}) + V_2(\vec{r})$$

$V_m(\vec{r})$ denotes the muffin-tin part of the potential and $V_1(\vec{r})+V_2(\vec{r})$ is the remainder.

In the preceding part of this chapter we gave a solution of the Hamiltonian, consisting of the first two terms. We study now the influence of the remaining part on the APW method.

$V_1(\vec{r})$ is defined to be zero inside the APW spheres, while $V_2(\vec{r})$ is zero outside. The influence of $V_1(\vec{r})$ can be treated simply and exactly, while $V_2(\vec{r})$ can be handled only approximately by perturbation theory. DeCicco (11) has found numerically, that the influence of $V_2(\vec{r})$ is negligible, so from now on we disregard it.

As has been indicated by several authors (12,13), $V_1(\vec{r})$ can be included exactly in the APW method. All that is needed is the addition of the matrix element of V_1, viz.

$$\langle i|V_1(\vec{r})|j\rangle = \int^{cell} \exp(-i\vec{k}_i.\vec{r})V_1(\vec{r})\exp(i\vec{k}_j.\vec{r})dv$$

$$= \Omega c(\vec{k}_i-\vec{k}_j)$$

to the original matrix element $(H-E)_{ij}$. Ω represents the volume

† *The Fourier coefficients are calculated in subroutine* FCOEFF *of program* MTPOT. *Program* (S)APW *has been extended by subroutine* V1MEP *to incorporate the Fourier coefficients.*

of the unit cell and $c(\vec{k}_i-\vec{k}_j)$ is the Fourier coefficient of $V_l(\vec{r})$ corresponding to the reciprocal lattice vector $(\vec{k}_i-\vec{k}_j)$ $(=\vec{K}_m)$.

We remark finally, that the Fourier series expansion of $V_l(\vec{r})$ converges very slowly, since this function is discontinuous at the APW spheres. However, this does not cause trouble, since the number of required Fourier coefficients is limited by the number of APW's needed to obtain sufficient convergence of the band energies.

3.9 THE FOLLOWED SCHEME FOR VO

The crystal structure of VO is fcc (see figure 3.2), so it has the same structure as rocksalt (NaCl). The space group is O_h^5.

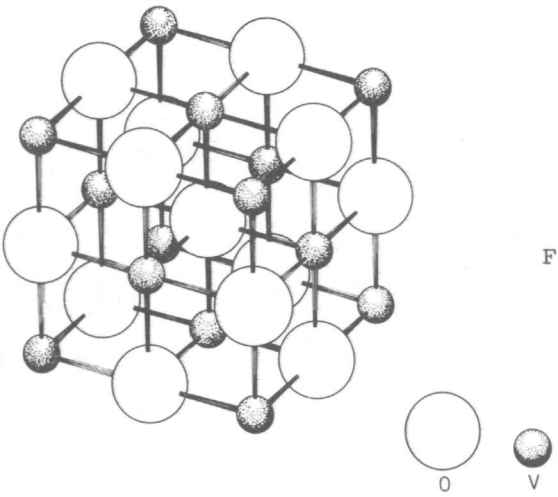

Fig. 3.2 The crystal structure of VO.

It is easy to construct the reciprocal lattice of this structure. The reciprocal lattice has the bcc structure, the first Brillouin zone is shown in figure 3.1 (see further paragraph 3.5).

We decide to restrict the calculation to the $\vec{k}$-points Γ, $\Delta(0,0,2)$, $\Delta(0,0,4)$, $\Delta(0,0,6)$, X, W, $\Sigma(0,2,2)$, $\Sigma(0,4,4)$, K, $\Lambda(2,2,2)$ and L.

The lattice constant a of VO has not been unambiguously determined. Several experimentalists (14-16) found different lattice constants. This is comprehensible if we realize, that VO

has a large number of vacancies (≃15%), which can vary dependent upon the conditions the substance has been prepared. Besides non-stoichiometry may be involved. We will rely on the work of Taylor *et al.* (16). Their results are very extensive in relation to those of others. They have determined the lattice constant as a function of the temperature, thereby giving information about the percentage of vacancies. The lattice constant varies roughly from 7.6 to 7.8 au. For that reason, we execute band structure calculations for four lattice constants (viz. 7.327, 7.677, 7.735 and 8.085 au), that is two constants within the mentioned range and two outside.

We make now some remarks about the determination of the radii of the muffin-tin spheres R_n. Suppose that the lattice is constituted of atoms A and B. Along the shortest distance between the atoms A and B, the muffin-tin potential is calculated by the α-Löwdin method, including both the Coulomb and the exchange part.

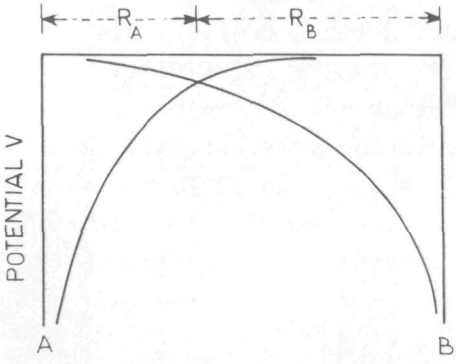

Fig. 3.3 The determination of the radii of the muffin-tin spheres.

The distance, where the potentials cross each other, determines the radii R_A and R_B as is shown in figure 3.3.

The crystal potential is, according to paragraph 3.6, a superposition of atomic potentials. An important question is what configuration to chose for the individual atoms or ions that constitute the lattice. According to classical electrostatic theory, VO consists of V^{2+} and O^{2-} ions. From the calculational point of view, however, it is impossible to calculate the atomic potential of O^{2-}, so we disregard the configuration (V^{2+},O^{2-}). Among others, Mattheiss (17) asserts, that it makes nearly no

difference whether the neutral or any ionic configuration is chosen. After all, the ionic nature of a crystal is not very well defined and may be ascribed both to charge transfer and to overlap effects. Especially the vanadium 4s electrons play herein an important role, since their average distance to the vanadium nucleus is rather large. Chosing a neutral configuration has the advantage that deviations of the muffin-tin potential are easily incorporated. The ground state of the neutral vanadium atom is $(3d)^3(4s)^2$ (see Moore (18)). Given the great radius of the 4s orbitals, this would lead to an effective charge close to +2 inside the vanadium muffin-tin spheres. According to various authors (19,20), better results are obtained with the configuration $(3d)^4 4s$, corresponding to a substantially lower positive charge within the vanadium muffin-tin spheres. For oxygen the configuration $(2p)^4$ is assumed.

The electron charge densities of the atoms, which are necessary for the calculation of the muffin-tin potential, are obtained by the Dirac-Slater method * (21), where relativistic effects have been neglected by substituting for the velocity of light the value $c = 10^8$ au. Since we intend to start with the crystal having the lattice constant $a = 7.735$ au (22), it is useful to shift the energy scales of the other calculations in such a way, that the constant muffin-tin potential (muffin-tin zero) has the same value. This makes a comparison between the different cases possible.

The effect of the deviation of the muffin-tin potential in the region outside the spheres is incorporated by developing that deviation in a Fourier series (see paragraph 3.8). The calculation of the Fourier coefficients consumes rather much computer time, since it is an integration of the superposed potential minus the muffin-tin potential on a three dimensional mesh. In order to have rather reliable coefficients, we calculate them with a Simpson rule on a mesh equivalent to 128,000 points in the entire

* *Dr.D.A.Liberman sent us the computer program, which uses the Dirac-Slater method for atoms and ions (see further Appendix II).*

unit cell. It is instructive to compare it with the way in which Mattheiss (23) calculated the Fourier coefficients for ReO_3. His integration has been executed with a rectangle rule over a three dimensional grid of points equivalent to 17,576 points in the entire unit cell.

Once the muffin-tin potential is known, the APW eigenvalues for the considered $\vec{k}$-points can be calculated. An important step in the APW calculation is the procedure to obtain the logarithmic derivative of the radial part of the wave function on the muffin-tin spheres. We use the procedure of Koelling* (24), whose method is especially suitable for a relativistic calculation. He decouples the matrix elements of the single particle Dirac equation for the periodic potential of the muffin-tin form in a non-relativistic analogon M^{NR} and a part M^{SO}, which contains the spin-orbit terms. The matrix elements M^{NR} contain the mass-velocity and the Darwin term. They equal exactly the non-relativistic elements if $c \to \infty$. It is hence possible to incorporate in this way all relativistic effects, except spin-orbit coupling. We simply substitute for $u'_l(R_n;E)/u_l(R_n;E)$ of paragraph 3.7, in the APW equations the analogical relativistic terms. In order to make comparison possible with other non-relativistic calculations, we eliminate, however, the relativistic effects by substituting $c = 10^8$ au.

According to paragraph 3.7, the wave function used is expanded in APW's characterized by the wave vectors $\vec{k}_i = \vec{k} + \vec{K}_i$. Including all APW's with wave vectors $\vec{k}_i$ with the property $|\vec{k}_i| \geq \sqrt{80}(\pi/a)$, will result in an eigenvalue accuracy of about 0.003 Ry (25). This corresponds to 113 unsymmetrized APW's at the Γ-point in $\vec{k}$-space. The APW matrix elements consist of an infinite summation over l from zero to infinity. We cut off the expansion in l at the value 12, since an upper limit $l = 18$ has shown to result in the same eigenvalues (25).

* *From Dr.D.D.Koelling we obtained the subroutine* DLGKAP *to calculate the logarithmic derivatives (see further Appendix II).*

REFERENCES

1. BORN M. and VON KARMAN T., *Phys. Z.* 13, 297 (1912)
2. JANSEN L. and BOON M., *Theory of finite groups*, North Holland, Amsterdam (1967)
3. SLATER J.C., *Phys. Rev.* 51, 846 (1937)
4. SLATER J.C. and DeCicco P.D., *Mass. Inst. Technol., Solid State and Molecular Theory Group. Quart. Progr. Rept.* No. 50 (1963)
5. HERMAN F. and SKILLMAN S., *Atomic Structure Calculations.* Prentice-Hall, Englewood Cliffs, New Yersey (1963)
6. LIBERMAN D., WABER J.T. and CROMER D.T., *Phys. Rev.* 137, A27 (1965)
7. LOWDIN P.O., *Advan. Phys.* 5, 1 (1956)
8. SLATER J.C., *Phys. Rev.* 81, 385 (1951)
9. SLATER J.C. and WOOD J.H., *Int. J. Quant. Chem.* 4, 3 (1971)
10. HAM F.S. and SEGALL B., *Phys. Rev.* 124, 1786 (1961)
11. DECICCO P.D., *Phys. Rev.* 153, 931 (1967)
12. SCHLOSSER H. and MARCUS P.M., *Phys. Rev.* 131, 2529 (1963)
13. BELEZNAY F. and LAWRENCE M.J., *J. Phys. C* 1, 1288 (1968)
14. PEARSON W.B., *A Handbook of Lattice Spacings and Structure of Metals and Alloys.* Pergamon Press, New York (1958)
15. WESTMAN S. and NORDMARK C., *Acta Chem. Scand.* 14, 465 (1960)
16. TAYLOR A. and DOYLE N.J., *J. Appl. Cryst.* 4, 103 (1971)
17. MATTHEISS L.F., *Phys. Rev.* B 5, 290 (1972)
18. MOORE C.E., *Atomic Energy Levels*, Vol. I, National Bureau of Standards, Circular No. 467, U.S. Government Printing Office, Washington D.C. (1949)
19. MATTHEISS L.F., *Phys. Rev.* 134, A970 (1964)
20. PAPACONSTANTOPOULOS D.A., ANDERSON J.R. and MC CAFFREY J.W., *Phys. Rev.* B 5, 1214 (1972)
21. see ref. 6
22. KRAAN D.J., *Phys. Status Solidi (b)* 60, -- (1973)
23. MATTHEISS L.F., *Phys. Rev.* 181, 987 (1969)
    ----------, *Phys. Rev.* B 2, 3918 (1970)
24. KOELLING D.D., *Phys. Rev.* 188, 1049 (1969)
25. ERN V. and SWITENDICK A.C., *Phys. Rev.* 137, A1927 (1965)

CHAPTER IV - BAND STRUCTURE CALCULATIONS

- LCAO INTERPOLATION -

4.1 INTRODUCTION

In the preceding chapter we have discussed the APW method. This method calculates the energy eigenvalues of a crystal for some $\vec{k}$-points in the Brillouin zone. The other eigenvalues $E(\vec{k})$ are then obtained by interpolation. One of the best interpolation schemes is the so-called LCAO interpolation method. This is not a purely mathematical device, but still is based on underlying chemical principles. Thus it will enable us to calculate the crystal-field parameter Δ when the valence electrons are localized.

4.2 THE LCAO INTERPOLATION SCHEME

As was shown in the preceding chapter, the general form of the wave function related to the periodic potential of a solid is of the Bloch type. One of the first proposed Bloch type orbitals is the linear combination of atomic orbitals (LCAO) (1). Such an LCAO wave function has the form:

$$\phi_{pq}(\vec{k},\vec{r}) = \frac{1}{\sqrt{N}} \sum_{\nu} \psi_p(\vec{r}-\vec{t}_\nu-\vec{\tau}_q)\exp\{i\vec{k}.(\vec{t}_\nu+\vec{\tau}_q)\}$$

where the sum is over all N lattice vectors $\vec{t}_\nu$ in the crystal. $\vec{\tau}_q$ is the position in the cell, with respect to the origin, of the q'th type of atom with the atomic wave function ψ_p, where p represents the atomic quantum numbers. The final wave function is a linear combination of the Bloch functions:

$$\Phi(\vec{k},\vec{r}) = \sum_{p,q} c_{pq}(\vec{k})\phi_{pq}(\vec{k},\vec{r}) \quad .... \quad \{1\}$$

The energy eigenvalues and the expansion coefficients $c_{pq}(\vec{k})$ are obtained by solving the secular equation:

$$\|H_{ij}(\vec{k}) - ES_{ij}(\vec{k})\| = 0$$

where each index i and j stands for the labels p and q. The overlap and transfer integrals are given by:

$$S_{ij}(\vec{k}) = e^{i\vec{k}.(\vec{\tau}_j-\vec{\tau}_i)} \sum_{\nu} e^{i\vec{k}.\vec{t}_\nu} \langle \psi_p(\vec{r}-\vec{\tau}_i) | \psi_{p'}(\vec{r}-\vec{t}_\nu-\vec{\tau}_j) \rangle$$

$$H_{ij}(\vec{k}) = e^{i\vec{k}.(\vec{\tau}_j-\vec{\tau}_i)} \sum_{\nu} e^{i\vec{k}.\vec{t}_\nu} \langle \psi_p(\vec{r}-\vec{\tau}_i) | H | \psi_{p'}(\vec{r}-\vec{t}_\nu-\vec{\tau}_j) \rangle$$

In the ab-initio LCAO method the overlap and transfer integrals are calculated directly, while a limited base set of atomic orbitals $\psi_p(\vec{r}-\vec{\tau}_i)$ is chosen. It is also clear that in that case the summation over the lattice vectors $\vec{t}_\nu$ is limited to the near neighbours. Ziman (2) argues that the LCAO method converges badly if the considered crystal contains "nearly free electrons" that is to say valence s and p electrons.

However, this LCAO method satisfies very well as an interpolation scheme (3). In that case the overlap and transfer integrals are used as parameters. For these parameters such values are taken that the LCAO eigenvalues agree as well as possible with the APW (or any other accurate method) eigenvalues for a limited number of symmetry points in $\vec{k}$-space.

The wave functions $\psi_{pq}(\vec{k},\vec{r})$ do not form an orthonormal set. Löwdin (4) has shown a way of constructing orthogonalized atomic orbitals by taking linear combinations of the atomic orbitals $\psi_p(\vec{r}-\vec{t}_\nu-\vec{\tau}_i)$. Another group of orthogonalized atomic orbitals consists of the well-known Wannier functions (5). They are obtained in a quite different way, but Löwdin (4) has shown that there is a close connection between these two kind of orthogonalized functions. Taking the Löwdin orbitals results in zero overlap integrals in the above mentioned equations. So only the transfer integrals have to be adapted. This method is essentially the interpolation scheme of Slater and Koster (6). In a useful note in their paper they demonstrate that the Löwdin orbitals transform in the same way as the atomic orbitals from which they arise. We shall refer to this scheme as the LCOAO method or the linear combination of orthogonalized atomic orbitals.

Mattheiss (7), on the contrary, uses the atomic orbitals

as basis functions. This scheme is indicated as the LCAO method. Mattheiss claims that his LCAO method treats the crystal-field effects in a physically more significant way. Moreover, his method leads to more realistic LCAO or "tight-binding" parameters. Therefore Mattheiss' method is used in this thesis. A clear disadvantage of this method is not only that more parameters have to be adapted, but also that the diagonalization process is more elaborate.

The electrons we are mainly dealing with in a band structure calculation are the valence electrons, since the core electrons occupy almost the same states as in the free atoms. For vanadium oxide we concentrate on the 2s and 2p electrons belonging to oxygen, and the 3d and 4s electrons related to vanadium. We further assume in our case of VO that the overlap integrals in the expression for S_{ij} are non-zero only for the nearest neighbours. Concerning the transfer integrals in the formula for H_{ij}, the first and second nearest neighbours are included. In the mentioned formulas a vanadium atom is chosen as the centre of the coordinate system. In table 4.1 the considered basis functions are shown, while the related matrix elements are listed in table 4.2. We establish that there are 29 independent parameters, that is 21 transfer and 5 overlap integrals. $E_{\psi_1,\psi_1}(lmn)$ symbolizes the transfer integral

$$\int \psi_1^*(r) H \psi_1(\vec{r}-l\vec{a}_1-m\vec{a}_2-n\vec{a}_3)\,dv$$

and $S_{\psi_1,\psi_1}(lmn)$ is the corresponding overlap integral

$$\int \psi_1^*(\vec{r}) \psi_1(\vec{r}-l\vec{a}_1-m\vec{a}_2-n\vec{a}_3)\,dv$$

$\vec{a}_1$, $\vec{a}_2$ and $\vec{a}_3$ are the unit vectors of the coordinate system in units a.

4.3 THE DETERMINATION OF THE INTERPOLATION PARAMETERS

In our interpolation scheme 10 atomic orbitals have been included as basis functions. This results in a 10 by 10 secular

Table 4.1

Basis functions of the LCAO interpolation scheme for VO.

Basis set Type		No.	Origin
Ligand	s_a	1	$a(\frac{1}{2},0,0)$
	x	2	$a(\frac{1}{2},0,0)$
	y	3	$a(\frac{1}{2},0,0)$
	z	4	$a(\frac{1}{2},0,0)$
Metal	xy	5	$a(0,0,0)$
	yz	6	$a(0,0,0)$
	zx	7	$a(0,0,0)$
	$3z^2-r^2$	8	$a(0,0,0)$
	x^2-y^2	9	$a(0,0,0)$
	s_c	10	$a(0,0,0)$

Table 4.2

Matrix elements of the LCAO interpolation scheme for VO.
$\xi = \frac{1}{2}k_x a \quad \eta = \frac{1}{2}k_y a \quad \zeta = \frac{1}{2}k_z a$

a. Anion-anion interactions

$$H_{1,1} = E_{s_a,s_a}(000)+4E_{s_a,s_a}(\tfrac{1}{2}\tfrac{1}{2}0)(\cos\xi.\cos\eta+\cos\xi.\cos\zeta+\cos\eta.\cos\zeta)$$

$$H_{2,2} = E_{x,x}(000)+4E_{x,x}(\tfrac{1}{2}\tfrac{1}{2}0)(\cos\xi.\cos\eta+\cos\xi.\cos\zeta)+4E_{x,x}(0\tfrac{1}{2}\tfrac{1}{2})(\cos\eta.\cos\zeta)$$

$$H_{3,3} = E_{x,x}(000)+4E_{x,x}(\tfrac{1}{2}\tfrac{1}{2}0)(\cos\eta.\cos\zeta+\cos\xi.\cos\eta)+4E_{x,x}(0\tfrac{1}{2}\tfrac{1}{2})(\cos\xi.\cos\zeta)$$

$$H_{4,4} = E_{x,x}(000)+4E_{x,x}(\tfrac{1}{2}\tfrac{1}{2}0)(\cos\xi.\cos\zeta+\cos\eta.\cos\zeta)+4E_{x,x}(0\tfrac{1}{2}\tfrac{1}{2})(\cos\xi.\cos\eta)$$

$$H_{1,2} = 4iE_{s_a,x}(\tfrac{1}{2}\tfrac{1}{2}0)(\sin\xi.\cos\eta+\sin\xi.\cos\zeta)$$

$$H_{1,3} = -4iE_{s_a,x}(\tfrac{1}{2}\tfrac{1}{2}0)(\sin\eta.\cos\zeta+\sin\eta.\cos\xi)$$

$$H_{1,4} = -4iE_{s_a,x}(\tfrac{1}{2}\tfrac{1}{2}0)(\sin\zeta.\cos\xi+\sin\zeta.\cos\eta)$$

$$H_{2,3} = -4E_{x,y}(\tfrac{1}{2}\tfrac{1}{2}0)(\sin\xi.\sin\eta)$$

$$H_{2,4} = -4E_{x,y}(\tfrac{1}{2}\tfrac{1}{2}0)(\sin\xi.\sin\zeta)$$

$$H_{3,4} = -4E_{x,y}(\tfrac{1}{2}\tfrac{1}{2}0)(\sin\eta.\sin\zeta)$$

b. Cation-cation interactions

$$H_{5,5} = E_{xy,xy}(000)+4E_{xy,xy}(\tfrac{1}{2}\tfrac{1}{2}0)(\cos\xi.\cos\eta)+4E_{xy,xy}(0\tfrac{1}{2}\tfrac{1}{2})(\cos\xi.\cos\zeta+\cos\eta.\cos\zeta)$$

$$H_{6,6} = E_{xy,xy}(000)+4E_{xy,xy}(\tfrac{1}{2}\tfrac{1}{2}0)(\cos\eta.\cos\zeta)+4E_{xy,xy}(0\tfrac{1}{2}\tfrac{1}{2})(\cos\xi.\cos\eta+\cos\xi.\cos\zeta)$$

$$H_{7,7} = E_{xy,xy}(000)+4E_{xy,xy}(\tfrac{1}{2}\tfrac{1}{2}0)(\cos\xi.\cos\zeta)+4E_{xy,xy}(0\tfrac{1}{2}\tfrac{1}{2})(\cos\eta.\cos\zeta+\cos\xi.\cos\eta)$$

Table 4.2 (continued)

$$H_{8,8} = E_{3z^2-r^2,3z^2-r^2}(000)+4E_{3z^2-r^2,3z^2-r^2}(\tfrac{1}{2}\tfrac{1}{2}0)(\cos\xi.\cos\eta + \tfrac{1}{4}\cos\xi.\cos\zeta+\tfrac{1}{4}\cos\eta.\cos\zeta)+3E_{x^2-y^2,x^2-y^2}(\tfrac{1}{2}\tfrac{1}{2}0)\cos\zeta.(\cos\xi+\cos\eta)$$

$$H_{9,9} = E_{3z^2-r^2,3z^2-r^2}(000)+3E_{3z^2-r^2,3z^2-r^2}(\tfrac{1}{2}\tfrac{1}{2}0)\cos\zeta.(\cos\xi+\cos\eta) + 4E_{x^2-y^2,x^2-y^2}(\tfrac{1}{2}\tfrac{1}{2}0)(\cos\xi.\cos\eta+\tfrac{1}{4}\cos\xi.\cos\zeta+\tfrac{1}{4}\cos\eta.\cos\zeta)$$

$$H_{10,10} = E_{s_c,s_c}(000)+4E_{s_c,s_c}(\tfrac{1}{2}\tfrac{1}{2}0)(\cos\xi.\cos\eta+\cos\xi.\cos\zeta+\cos\eta.\cos\zeta)$$

$$H_{5,6} = -4E_{xy,xz}(0\tfrac{1}{2}\tfrac{1}{2})(\sin\xi.\sin\zeta)$$

$$H_{5,7} = -4E_{xy,xz}(0\tfrac{1}{2}\tfrac{1}{2})(\sin\eta.\sin\zeta)$$

$$H_{5,8} = -4E_{xy,3z^2-r^2}(\tfrac{1}{2}\tfrac{1}{2}0)(\sin\xi.\sin\eta)$$

$$H_{5,10} = -4E_{s_c,xy}(\tfrac{1}{2}\tfrac{1}{2}0)(\sin\xi.\sin\eta)$$

$$H_{6,7} = -4E_{xy,xz}(0\tfrac{1}{2}\tfrac{1}{2})(\sin\xi.\sin\eta)$$

$$H_{6,8} = +2E_{xy,3z^2-r^2}(\tfrac{1}{2}\tfrac{1}{2}0)(\sin\eta.\sin\zeta)$$

$$H_{6,9} = -2\sqrt{3}E_{xy,3z^2-r^2}(\tfrac{1}{2}\tfrac{1}{2}0)(\sin\eta.\sin\zeta)$$

$$H_{6,10} = -4E_{s_c,xy}(\tfrac{1}{2}\tfrac{1}{2}0)(\sin\eta.\sin\zeta)$$

$$H_{7,8} = +2E_{xy,3z^2-r^2}(\tfrac{1}{2}\tfrac{1}{2}0)(\sin\xi.\sin\zeta)$$

$$H_{7,9} = +2\sqrt{3}E_{xy,3z^2-r^2}(\tfrac{1}{2}\tfrac{1}{2}0)(\sin\xi.\sin\zeta)$$

$$H_{7,10} = -4E_{s_c,xy}(\tfrac{1}{2}\tfrac{1}{2}0)(\sin\xi.\sin\zeta)$$

$$H_{8,9} = +\sqrt{3}E_{3z^2-r^2,3z^2-r^2}(\tfrac{1}{2}\tfrac{1}{2}0)(\cos\xi.\cos\zeta-\cos\eta.\cos\zeta) - \sqrt{3}E_{x^2-y^2,x^2-y^2}(\tfrac{1}{2}\tfrac{1}{2}0)(\cos\xi.\cos\zeta-\cos\eta.\cos\zeta)$$

$$H_{8,10} = -2E_{s_c,3z^2-r^2}(\tfrac{1}{2}\tfrac{1}{2}0)(-2\cos\xi.\cos\eta+\cos\xi.\cos\zeta+\cos\eta.\cos\zeta)$$

$$H_{9,10} = +2\sqrt{3}E_{s_c,3z^2-r^2}(\tfrac{1}{2}\tfrac{1}{2}0)(-\cos\xi.\cos\zeta+\cos\eta.\cos\zeta)$$

---

c. Cation-anion interactions

$$H_{1,8} = E_{s_a,3z^2-r^2}(00\tfrac{1}{2})(-\cos\xi-\cos\eta+2\cos\zeta)$$

$$H_{1,9} = \sqrt{3}E_{s_a,3z^2-r^2}(00\tfrac{1}{2})(\cos\xi-\cos\eta)$$

$$H_{1,10} = 2E_{s_c,s_a}(\tfrac{1}{2}00)(\cos\xi+\cos\eta+\cos\zeta)$$

$$H_{2,5} = 2iE_{x,xy}(0\tfrac{1}{2}0)(\sin\eta)$$

$$H_{2,7} = 2iE_{x,xy}(0\tfrac{1}{2}0)(\sin\zeta)$$

$$H_{2,8} = -iE_{z,3z^2-r^2}(00\tfrac{1}{2})(\sin\xi)$$

$$H_{2,9} = \sqrt{3}iE_{z,3z^2-r^2}(00\tfrac{1}{2})(\sin\xi)$$

$$H_{2,10} = -2iE_{s_c,x}(\tfrac{1}{2}00)(\sin\xi)$$

$$H_{3,5} = 2iE_{x,xy}(0\tfrac{1}{2}0)(\sin\xi)$$

$$H_{3,6} = 2iE_{x,xy}(0\tfrac{1}{2}0)(\sin\zeta)$$

$$H_{3,8} = -iE_{z,3z^2-r^2}(00\tfrac{1}{2})(\sin\eta)$$

$$H_{3,9} = -\sqrt{3}iE_{z,3z^2-r^2}(00\tfrac{1}{2})(\sin\eta)$$

$$H_{3,10} = -2iE_{s_c,x}(\tfrac{1}{2}00)(\sin\eta)$$

$$H_{4,6} = 2iE_{x,xy}(0\tfrac{1}{2}0)(\sin\eta)$$

$$H_{4,7} = 2iE_{x,xy}(0\tfrac{1}{2}0)(\sin\xi)$$

$$H_{4,8} = 2iE_{z,3z^2-r^2}(00\tfrac{1}{2})(\sin\zeta)$$

$$H_{4,10} = -2iE_{s_c,x}(\tfrac{1}{2}00)(\sin\zeta)$$

determinant to be solved at every desired $\vec{k}$-point. As pointed out in the preceding chapter, it is advantageous to make use of the symmetry of specific $\vec{k}$-vectors we like to consider. We concentrate therefore on the "little group" $G_{\vec{k}}$ of these $\vec{k}$-vectors. Denoting the elements of $G_{\vec{k}}$ by R we can write the projection operator for the α'th irreducible representation of $G_{\vec{k}}$ as

$$\rho^{\alpha}_{lj} = \sum_{R} \{\Gamma^{\alpha}_{lj}(R)\}^{*} R$$

$\Gamma^{\alpha}_{lj}(R)$ is the lj'th element of the matrix corresponding to the operator R in the α'th irreducible representation of $G_{\vec{k}}$. Application of this projection operator leads to a basis function for the irreducible representation α:

$$\chi^{\alpha}_{i'lj}(\vec{k},\vec{r}) = \rho^{\alpha}_{lj}\phi_{pq}(\vec{k},\vec{r})$$

i' stands for the indices p and q. Introducing the expression for ρ^{α}_{lj} leads to:

$$\chi^{\alpha}_{i'lj}(\vec{k},\vec{r}) = \sum_{R}\sum_{\nu} \exp(i\vec{k}.(\vec{t}_{\nu}+\vec{\tau}_{q}))\,(\Gamma_{lj}(R))^{*} \times \{R\psi_{p}(R(\vec{r}-\vec{t}_{\nu}-\vec{\tau}_{q}))\}$$

$$= \sum_{\nu} \exp(i\vec{k}.(\vec{t}_{\nu}+\vec{\tau}_{q})) \sum_{R} \exp(-i\vec{k}.\vec{t}_{R}) \times (\Gamma_{lj}(R))^{*}(R\psi_{p}(\vec{r}-\vec{t}_{\nu}-\vec{\tau}_{q_R}))$$

$\vec{\tau}_{q_R}$ originates from the unique relation:

$$R\vec{\tau}_{q} = \vec{t}_{R} + \vec{\tau}_{q_R}$$

$\vec{t}_{R}$ is a translation vector and $\vec{\tau}_{q_R}$ refers to the atomic coordinates in the cell (8).

In the rocksalt structure it is evident that:

$$\vec{\tau}_{1_R} = \vec{\tau}_{1} = (0,0,0)a \quad \text{and} \quad \vec{\tau}_{2_R} = \vec{\tau}_{2} = (\tfrac{1}{2},0,0)a$$

The index 1 refers to vanadium and the index 2 to oxygen. The use of symmetrized orbitals has the advantage that orbitals, belonging to different representations, do not admix with each other. Hence, the 10 by 10 secular determinant will be subdivided in smaller determinants. We restrict ourselves to the $\vec{k}$-points Γ, $\Delta(0,0,2)$,

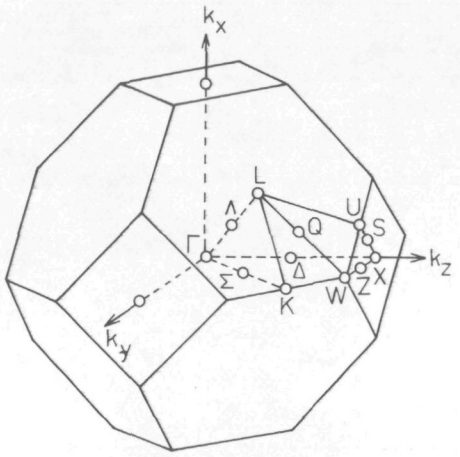

Fig. 4.1 The first Brillouin zone of fcc VO.

$\Delta(0,0,4)$, $\Delta(0,0,6)$, X, W, $\Sigma(0,2,2)$, $\Sigma(0,4,4)$, K, $\Lambda(2,2,2)$ and L (see figure 4.1). The figures between parentheses indicate the $\vec{k}$-vector in units $\pi/4a$. Application of the projection operator formalism for the considered $\vec{k}$-points gives results as shown in table 4.3. In assembling this table, the convention of Cornwell (9) has been used, since he has already projected out some spherical harmonics for several cubic space groups.

Suppose now that an LCAO eigenvalue is denoted by ε_i, while the related APW eigenvalue is indicated by E_i. We require for the considered $\vec{k}$-points:

$$\sum_{i=1}^{m} w_i (E_i - \varepsilon_i)^2 \implies \text{minimum}$$

w_i is a weighing factor, which is necessary in order to obtain convergence in this least-squares procedure. Minimization is obtained by variation of the overlap and transfer integrals. Once we know the integrals, it is possible to determine the ε_i's for a

Table 4.3

Symmetrized wave functions for the rocksalt structure. The phase factors are not mentioned. The figures between parentheses indicate the centre of the function.

Representation	Row	Symmetrized functions
Γ_1	1	$s_a(\frac{1}{2}00)$; $s_c(000)$;
Γ_{12}	1	$x^2-y^2(000)$;
	2	$3z^2-r^2(000)$;
$\Gamma_{25'}$	1	$xy(000)$;
	2	$yz(000)$;
	3	$zx(000)$;
Γ_{15}	1	$x(\frac{1}{2}00)$;
	2	$y(\frac{1}{2}00)$;
	3	$z(\frac{1}{2}00)$;
Δ_1	1	$s_a(\frac{1}{2}00)$; $z(\frac{1}{2}00)$; $3z^2-r^2(000)$; $s_c(000)$;
Δ_2	1	$x^2-y^2(000)$;
$\Delta_{2'}$	1	$xy(000)$;
Δ_5	1	$x(\frac{1}{2}00)$; $zx(000)$;
	2	$y(\frac{1}{2}00)$; $yz(000)$;
X_1	1	$s_a(\frac{1}{2}00)$; $3z^2-r^2(000)$; $s_c(000)$;
X_2	1	$x^2-y^2(000)$;
X_3	1	$xy(000)$;
$X_{4'}$	1	$z(\frac{1}{2}00)$;
X_5	1	$yz(000)$;
	2	$-zx(000)$;
$X_{5'}$	1	$x(\frac{1}{2}00)$;
	2	$y(\frac{1}{2}00)$;

Table 4.3 (continued)

W_1	1	$y(\frac{1}{2}00)$; $\frac{1}{2}\{\sqrt{3}(x^2-y^2)+(3z^2-r^2)\}(000)$; $s_c(000)$;
$W_{1'}$	1	$zx(000)$;
$W_{2'}$	1	$s_a(\frac{1}{2}00)$; $\frac{1}{2}\{(x^2-y^2)-\sqrt{3}(3z^2-r^2)\}(000)$;
W_3	1	$x(\frac{1}{2}00)$; $xy(000)$;
	2	$z(\frac{1}{2}00)$; $-yz(000)$;
Σ_1	1	$s_a(\frac{1}{2}00)$; $\frac{1}{2}\sqrt{2}(y+z)(\frac{1}{2}00)$; $yz(000)$; $\frac{1}{2}\{\sqrt{3}(x^2-y^2)-(3z^2-r^2)\}(000)$; $s_c(000)$;
Σ_2	1	$\frac{1}{2}\sqrt{2}(xy-zx)(000)$;
Σ_3	1	$x(\frac{1}{2}00)$; $\frac{1}{2}\sqrt{2}(xy+zx)(000)$;
Σ_4	1	$\frac{1}{2}\sqrt{2}(y-z)(\frac{1}{2}00)$; $\frac{1}{2}\{(x^2-y^2)+\sqrt{3}(3z^2-r^2)\}(000)$;
K_1	1	$s_a(\frac{1}{2}00)$; $\frac{1}{2}\sqrt{2}(y+z)(\frac{1}{2}00)$; $yz(000)$; $\frac{1}{2}\{\sqrt{3}(x^2-y^2)-(3z^2-r^2)\}(000)$; $s_c(000)$;
K_2	1	$\frac{1}{2}\sqrt{2}(xy-zx)(000)$;
K_3	1	$x(\frac{1}{2}00)$; $\frac{1}{2}\sqrt{2}(xy+zx)(000)$;
K_4	1	$\frac{1}{2}\sqrt{2}(y-z)(\frac{1}{2}00)$; $\frac{1}{2}\{(x^2-y^2)+\sqrt{3}(3z^2-r^2)\}(000)$;
Λ_1	1	$s_a(\frac{1}{2}00)$; $(x+y+z)/\sqrt{3}(\frac{1}{2}00)$; $(xy+yz+zx)/\sqrt{3}(000)$; $s_c(000)$;
Λ_3	1	$\frac{1}{2}\sqrt{2}(x-y)(\frac{1}{2}00)$; $\frac{1}{2}\sqrt{2}(yz-zx)(000)$; $x^2-y^2(000)$;
	2	$(2z-x-y)/\sqrt{6}(\frac{1}{2}00)$; $(2xy-yz-zx)/\sqrt{6}(000)$; $3z^2-r^2(000)$;
L_1	1	$(x+y+z)/\sqrt{3}(\frac{1}{2}00)$; $(xy+yz+zx)/\sqrt{3}(000)$; $s_c(000)$;
L_3	1	$\frac{1}{2}\sqrt{2}(x-y)(\frac{1}{2}00)$; $\frac{1}{2}\sqrt{2}(yz-zx)(000)$; $(x^2-y^2)(000)$;
	2	$(x+y-2z)/\sqrt{6}(\frac{1}{2}00)$; $(2xy-yz-zx)/\sqrt{6}(000)$; $3z^2-r^2(000)$;
$L_{2'}$	1	$s_c(\frac{1}{2}00)$;

dense network in $\vec{k}$-space.

Since the 10 by 10 secular determinants are blocked out in 1 by 1 to 5 by 5 subdeterminants, we can expect that in general the dependence of the parameters ε_i on the transfer and overlap integrals is non-linear. This fact may cause difficulties in the least-squares procedure. Good starting values of the integrals are therefore indispensable. A method for determining these starting values is derived in Appendix I.

4.4 CRYSTAL-FIELD PARAMETERS

In the preceding pages, the overlap and transfer integrals have been defined. It is interesting to see how crystal-field parameters can be derived from the values of these overlap and transfer integrals.

In crystal-field theory the central ion (vanadium) is considered to be isolated. The influence of the surrounding ligands is incorporated by assuming that they cause an electric field. This electric field, which has the symmetry of the crystal, can split the orbitals of the central atom. So we are interested in knowing how the vanadium 3d orbitals split under the influence of the oxygen 2s and 2p orbitals. In this regard we follow Mattheiss (7) who used the perturbation theory of Löwdin (10). Formally, we start with the LCAO matrix formulation:

$$\begin{bmatrix} \underline{H}_{s_a s_a} & \underline{H}_{s_a p} & \underline{H}_{s_a d} & \underline{H}_{s_a s_c} \\ \underline{H}^{\dagger}_{s_a p} & \underline{H}_{pp} & \underline{H}_{pd} & \underline{H}_{ps_c} \\ \underline{H}^{\dagger}_{s_a d} & \underline{H}^{\dagger}_{pd} & \underline{H}_{dd} & \underline{H}_{ds_c} \\ \underline{H}^{\dagger}_{s_a s_c} & \underline{H}^{\dagger}_{ps_c} & \underline{H}^{\dagger}_{ds_c} & \underline{H}_{s_c s_c} \end{bmatrix} \begin{bmatrix} \vec{c}_{s_a} \\ \vec{c}_p \\ \vec{c}_d \\ \vec{c}_{s_c} \end{bmatrix} = \begin{bmatrix} E\underline{1} & \underline{0} & E\underline{S}_{s_a d} & E\underline{S}_{s_a s_c} \\ \underline{0} & E\underline{1} & E\underline{S}_{pd} & E\underline{S}_{ps_c} \\ E\underline{S}^{\dagger}_{s_a d} & E\underline{S}^{\dagger}_{pd} & E\underline{1} & \underline{0} \\ E\underline{S}^{\dagger}_{s_a s_c} & E\underline{S}^{\dagger}_{ps_c} & \underline{0} & E\underline{1} \end{bmatrix} \begin{bmatrix} \vec{c}_{s_a} \\ \vec{c}_p \\ \vec{c}_d \\ \vec{c}_{s_c} \end{bmatrix}$$

the eigenvector $\vec{C}$ has been decomposed into s_a, p, d and s_c components. The matrix equation is multiplied out, whereafter the vectors $\vec{c}_{s_a}$, $\vec{c}_p$ and $\vec{c}_{s_c}$ are eliminated. The above relation results then in the matrix equation:

$$\underline{H}'_{dd}\,\vec{C}_d = E\underline{1}\,\vec{C}_d$$

where $\underline{H}'_{dd} = \underline{H}_{dd} + (\underline{H}^{\dagger}_{s_a d} - E\underline{S}^{\dagger}_{s_a d})(E\underline{1} - \underline{H}_{s_a s_a})^{-1}(\underline{H}_{s_a d} - E\underline{S}_{s_a d})$

$$+ (\underline{H}^{\dagger}_{pd} - E\underline{S}^{\dagger}_{pd})(E\underline{1} - \underline{H}_{pp})^{-1}(\underline{H}_{pd} - E\underline{S}_{pd}) + \underline{H}^{\dagger}_{ds_c}(E\underline{1} - \underline{H}_{s_c s_c})^{-1}\underline{H}_{ds_c}$$

+ higher order matrix terms.

We neglect the higher order matrix terms and define

$$\underline{\Delta}^{\alpha}_{dd} \equiv (\underline{H}^{\dagger}_{\alpha d} - E\underline{S}^{\dagger}_{\alpha d})(E\underline{1} - \underline{H}_{\alpha\alpha})^{-1}(\underline{H}_{\alpha d} - E\underline{S}_{\alpha d})$$

This results in: $\underline{H}'_{dd} = \underline{H}_{dd} + \underline{\Delta}^{s_a}_{dd} + \underline{\Delta}^{p}_{dd} + \underline{\Delta}^{s_c}_{dd}$

Dividing $\underline{H}_{\alpha\alpha}$ in its diagonal and non-diagonal parts, $E_\alpha\underline{1}$ and $\underline{H}^{nd}_{\alpha\alpha}$, and expanding $(E\underline{1} - E_\alpha\underline{1} - \underline{H}^{nd}_{\alpha\alpha})^{-1}$ in a power series in $\underline{H}^{nd}_{\alpha\alpha}$, we obtain:

$$\underline{\Delta}^{\alpha}_{dd} = (\underline{H}^{\dagger}_{\alpha d} - E\underline{S}^{\dagger}_{\alpha d})(E\underline{1} - E_\alpha\underline{1})^{-1}(\underline{H}_{\alpha d} - E\underline{S}_{\alpha d})$$

$$+ (\underline{H}^{\dagger}_{\alpha d} - E\underline{S}^{\dagger}_{\alpha d})(E\underline{1} - E_\alpha\underline{1})^{-1}(\underline{H}^{nd}_{\alpha\alpha})(E\underline{1} - E_\alpha\underline{1})^{-1}(\underline{H}_{\alpha d} - E\underline{S}_{\alpha d}) + \ldots$$

We retain only the first term in this expansion and substitute for the energy E the eigenvalues E_d, so the mentioned equations reduce to a second order perturbation theory approximation. It is now possible to calculate the matrix elements of the effective d block.

Now we make a step toward the crystal-field theory in the localized case. Anderson (11) has shown that the energy of the localized Wannier (5) functions is equal to the *average* energy of the corresponding band. In an octahedral field the d functions of the central vanadium atom are split into e_g and t_{2g} orbitals. By averaging over $\vec{k}$-space, the energy for the e_g states $\langle E_e \rangle$ turns up as:

$$\langle E_e \rangle = E_{3z^2-r^2,3z^2-r^2}(000) + \tfrac{1}{2}(\Delta_{s_a} + \Delta_\sigma + \Delta_{s_c})$$

For the t_{2g} band we get:

$$\langle E_t \rangle = E_{xy,xy}(000) + \tfrac{1}{2}(\Delta_\pi + \Delta'_{s_c})$$

The crystal-field parameters Δ_{s_a}, Δ_π, Δ_σ, Δ''_{s_c} and Δ'_{s_c} are determined from the LCAO parameters by the relations:

$$\Delta_{s_a} = \frac{6\left[E_{s_a,3z^2-r^2}(00\tfrac{1}{2}) - E_{3z^2-r^2,3z^2-r^2}(000) S_{s_a,3z^2-r^2}(00\tfrac{1}{2})\right]^2}{E_{3z^2-r^2,3z^2-r^2}(000) - E_{s_a,s_a}(000)}$$

$$\Delta_\pi = \frac{8\left[E_{x,xy}(0\tfrac{1}{2}0) - E_{xy,xy}(000) S_{x,xy}(0\tfrac{1}{2}0)\right]^2}{E_{xy,xy}(000) - E_{x,x}(000)}$$

$$\Delta_\sigma = \frac{6\left[E_{z,3z^2-r^2}(00\tfrac{1}{2}) - E_{3z^2-r^2,3z^2-r^2}(000) S_{z,3z^2-r^2}(00\tfrac{1}{2})\right]^2}{E_{3z^2-r^2,3z^2-r^2}(000) - E_{x,x}(000)}$$

$$\Delta''_{s_c} = \frac{8\left[E_{s_c,xy}(\tfrac{1}{2}\tfrac{1}{2}0)\right]^2}{E_{xy,xy}(000) - E_{s_c,s_c}(000)}$$

$$\Delta'_{s_c} = \frac{12\left[E_{s_c,3z^2-r^2}(\tfrac{1}{2}\tfrac{1}{2}0)\right]^2}{E_{3z^2-r^2,3z^2-r^2}(000) - E_{s_c,s_c}(000)}$$

So in the localized limit the e_g and t_{2g} orbitals undergo a splitting Δ (=10Dq), which is defined as:

$$\langle E_e \rangle - \langle E_t \rangle = E_{3z^2-r^2,3z^2-r^2}(000) - E_{xy,xy}(000)$$

$$+ \tfrac{1}{2}\{\Delta_{s_a} + \Delta_\sigma + \Delta''_{s_c} - \Delta_\pi - \Delta'_{s_c}\}$$

This result is illustrated by figure 4.2. We remark that, for example, $E(t_{2g})$ on the left side equals $E_{xy,xy}(000)$, while analogous statements hold for the other levels.

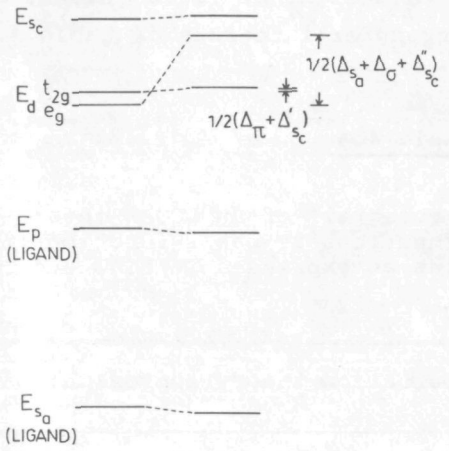

Fig. 4.2 Orbital splitting in an octahedral field.

Mattheiss (12) asserts that if the lattice periodicity is taken into account the e_g bandwidth is $(\Delta_\sigma + \Delta_{s_a})$, while the width of the t_{2g} band is equal to Δ_π, provided that the d bands are sufficiently narrow and the crystal field sufficiently strong. Actually, however, the interaction between the metal atoms has about the same magnitude as the crystal-field parameters. Therefore it is better to express the width of the t_{2g} band as:

$$W_{t_{2g}} = E(X_5) - E(X_3) = 8\left(E_{xy,xy}(0\tfrac{1}{2}\tfrac{1}{2}) - E_{xy,xy}(\tfrac{1}{2}\tfrac{1}{2}0)\right)$$

In the transition metal oxide series, as calculated by Mattheiss (12), the t_{2g} band is the broadest band. The e_g band is normally much smaller and cannot be easily written down in LCAO parameters.

The perturbation theory approximation of the crystal-field parameters gives us a qualitative insight. Because of the approximations involved, numerical data should be considered with a great deal of caution. It can therefore be advisable to make an independent calculation of the crystal-field parameter Δ along a different route. To this end we have adapted the APW results of the vanadium 3d bands by an LCOAO interpolation scheme. That is, five 3d Bloch orbitals, each constructed from the Löwdin orthogonalized 3d functions, are used as a basis set. Incorporating the

vanadium nearest- and second nearest-neighbour interactions, results in the twelve independent transfer integrals of table 4.4.

Table 4.4

Relation between the transfer integrals of an LCOAO interpolation scheme, with only d functions as basis functions, and the corresponding quantities as expressed in LCAO and crystal-field parameters.

Effective parameter	Perturbation theory approximation
$\varepsilon_{xy,xy}(000)$	$E_{xy,xy}(000) + \frac{1}{2}(\Delta_\pi+\Delta'_{s_c})$
$\varepsilon_{xy,xy}(\frac{1}{2}\frac{1}{2}0)$	$E_{xy,xy}(\frac{1}{2}\frac{1}{2}0)$
$\varepsilon_{xy,xy}(0\frac{1}{2}\frac{1}{2})$	$E_{xy,xy}(0\frac{1}{2}\frac{1}{2})$
$\varepsilon_{xy,xz}(0\frac{1}{2}\frac{1}{2})$	$E_{xy,xz}(0\frac{1}{2}\frac{1}{2}) - (\Delta_\pi+2\Delta'_{s_c})/8$
$\varepsilon_{xy,xy}(100)$	$E_{xy,xy}(100)^\dagger - (\Delta_\pi+2\Delta'_{s_c})/8$
$\varepsilon_{xy,xy}(001)$	$E_{xy,xy}(001)^\dagger$
$\varepsilon_{3z^2-r^2,3z^2-r^2}(000)$	$E_{3z^2-r^2,3z^2-r^2}(000) + \frac{1}{2}(\Delta_{s_a}+\Delta_\sigma+\Delta''_{s_c})$
$\varepsilon_{3z^2-r^2,3z^2-r^2}(\frac{1}{2}\frac{1}{2}0)$	$E_{3z^2-r^2,3z^2-r^2}(\frac{1}{2}\frac{1}{2}0) + (3\Delta_{s_a}+\Delta''_{s_c})/36$
$\varepsilon_{x^2-y^2,x^2-y^2}(\frac{1}{2}\frac{1}{2}0)$	$E_{x^2-y^2,x^2-y^2}(\frac{1}{2}\frac{1}{2}0) - (4\Delta_{s_a}+\Delta''_{s_c})/16$
$\varepsilon_{xy,3z^2-r^2}(\frac{1}{2}\frac{1}{2}0)$	$E_{xy,3z^2-r^2}(\frac{1}{2}\frac{1}{2}0) - (3\Delta_\pi\Delta_\sigma)^{\frac{1}{2}}/12$
$\varepsilon_{3z^2-r^2,3z^2-r^2}(001)$	$E_{3z^2-r^2,3z^2-r^2}(001)^\dagger - (\Delta_\sigma-\Delta_{s_a})/6$
$\varepsilon_{x^2-y^2,x^2-y^2}(001)$	$E_{x^2-y^2,x^2-y^2}(001)^\dagger$

† These parameters are not included in the LCAO interpolation scheme.

Table 4.4 again illustrates the potential danger in ascribing too much physical importance to the LCAO interpolation parameters. In the transfer integrals anion-cation covalency contributions and cation-cation d band transfer integrals are involved and intermixed. Parameters, which are intended to represent a d-d interaction can easily be dominated by p-d or s-d contributions.

Calculations of parameters along LCAO and LCOAO lines have been performed. Results will be compared in chapter V. In order to judge further whether the so obtained crystal-field parameter Δ is sufficiently reliable, the LCOAO interpolation for the vanadium 3d bands has been repeated, whereby also the vanadium third nearest-neighbour interactions are included. This scheme results in 21 independent transfer integrals.

REFERENCES

1. BLOCH F., *Z. Physik* 52, 555 (1928)
2. ZIMAN J.M., In *Solid State Physics* (Edited by F.Seitz, D.Turnbull and H.Ehrenreich), Vol. 26, p. 1, Academic Press, New York (1971)
3. CONNOLLY J.W.D., In *Proceedings of Electronic Density of States Symposium*, NBS, Gaithersburg, Md. (1969)
4. LOWDIN P.O., *J. Chem. Phys.* 18, 365 (1950)
5. WANNIER G.H., *Phys. Rev.* 52, 191 (1937)
6. SLATER J.C. and KOSTER G.F., *Phys. Rev.* 94, 1498 (1954)
7. MATTHEISS L.F., *Phys. Rev.* B 2, 3918 (1970)
8. FLODMARK S., *Technical Report No. 1*, Institute of Theoretical Physics, University of Stockholm, Stockholm, Sweden
9. CORNWELL J.F., *Group Theory and Electronic Energy Bands in Solids*, North Holland, Amsterdam (1969)
10. LOWDIN P.O., *J. Chem. Phys.* 19, 1396 (1951)
11. ANDERSON P.W., In *Solid State Physics* (Edited by F.Seitz and D.Turnbull), Vol. 14, p. 155, Academic Press, New York (1963)
12. MATTHEISS L.F., *Phys. Rev.* B 5, 290 (1972)

note: The computer programs, which execute the LCAO interpolation scheme, viz. STARTVAL, MINLEIGV *and* INTERPOLATE, *have been developed in the course of this work (see further Appendix II).*

CHAPTER V - BAND STRUCTURE CALCULATIONS

- RESULTS -

5.1 INTRODUCTION

In the following pages, the results are presented of the combined APW-LCAO calculations on VO. The study of the eventually semiconductor-metal transition and the calculation of the crystal-field parameter of V^{2+} in MgO compel us to execute a calculation for several lattice distances a, viz. 7.327, 7.677, 7.735 and 8.085 au. We indicate these different cases by resp. I, II, III and IV.

5.2 THE MUFFIN-TIN POTENTIAL

A survey of the muffin-tin potential calculations is given

Table 5.1

Some results of the muffin-tin potential calculation on VO. I, II, III and IV refer to the respectively lattice constants 7.327, 7.677, 7.735 and 8.085 au.

	units	I	II	III	IV
Lattice parameter a	au	7.327	7.677	7.735	8.085
APW radius R_V of vanadium	au	1.929	2.053	2.053	2.118
APW radius R_O of oxygen	au	1.702	1.756	1.812	1.869
Constant Coulomb potential	Ry	-0.823	-0.676	-0.654	-0.549
Constant exchange potential	Ry	-1.045	-0.965	-0.947	-0.885
Muffin-tin zero V_c	Ry	-1.867	-1.641	-1.601	-1.434
Electron charge within vanadium muffin-tin sphere	au	21.46	21.64	21.62	21.64
Electron charge within oxygen muffin-tin sphere	au	7.439	7.472	7.587	7.618

in table 5.1. These data are related to the situation before the energy shift of the muffin-tin zero. The APW radii R_V for the cases II and III have the same value because we let coincide the APW radius with a meshpoint of a rather coarse logarithmic scale. It is evident that in this case too the different spheres don't overlap each other. We notice that the superposition of Coulomb potentials or atomic charges includes 320 like and 370 unlike atoms in our calculations. If the potential within the vanadium muffin-tin spheres is calculated, vanadium is the like atom and oxygen the unlike one and so on.

An interesting point is to compare the charges with those obtained by Neckel (1). He has executed a self-consistent APW calculation on VO with a lattice constant a = 7.736 au, hence it is best comparable with case III. Neckel takes for the muffin-tin radii R_V and R_O the respective values 2.0789 and 1.7885 au. He starts with a neutral atom configuration. The starting values of the electron charge are 21.21 and 7.45 au respectively. At the end of the calculation, these values are 20.98 and 7.93 au. The small shift in the charge justifies the use of the neutral atom configuration.

Comparison of the absolute values of the charges should be taken not too seriously, since Neckel (1) uses for the exchange approximation the Xα method (2), while in our work Slater full exchange is applied.

5.3 THE APW CALCULATION

The results of the APW calculation of VO are summarized in table 5.2. We call to mind that the energy scales are shifted in such a way that all muffin-tin zeros equal the value -1.601 of case III. For the lattice constant a = 7.735 au, the APW eigenvalues, as a function of the $\vec{k}$-vector for some symmetry directions, are illustrated by figure 5.1

The comparison between the different cases is made clear by figure 5.2, where the APW eigenvalues along the Δ-axis are shown.

The APW eigenvalues are calculated, as mentioned, in a non-

Table 5.2

APW and LCAO energy eigenvalues. The wave vector $\vec{k}$ is indicated in units $\pi/4a$, the energy eigenvalues are expressed in Rydberg units. The symbols following the coordinates of the $\vec{k}$-points are the irreducible representations.

		I		II		III		IV	
$\vec{k}$		APW	LCAO	APW	LCAO	APW	LCAO	APW	LCAO
000	Γ_1	1.012	1.013	0.980	0.981	0.976	0.976	0.956	0.950
		-1.224	-1.226	-1.099	-1.102	-1.081	-1.087	-0.980	-0.983
	Γ_{15}	0.038	0.036	0.132	0.133	0.145	0.148	0.220	0.221
	$\Gamma_{25'}$	0.775	0.766	0.865	0.857	0.878	0.871	0.944	0.940
	Γ_{12}	0.898	0.899	0.966	0.966	0.975	0.972	1.025	1.021
002	Δ_1	1.088	1.185	1.067	1.156	1.067	1.145	1.078	1.130
		0.958	0.949	0.992	0.988	0.995	0.997	0.996	1.011
		-0.038	-0.036	0.072	0.070	0.088	0.082	0.174	0.173
		-1.199	-1.201	-1.082	-1.082	-1.065	-1.063	-0.969	-0.969
	Δ_2	0.910	0.914	0.975	0.978	0.984	0.984	1.032	1.031
	$\Delta_{2'}$	0.733	0.732	0.830	0.829	0.844	0.843	0.917	0.916
	Δ_5	0.830	0.828	0.908	0.907	0.920	0.918	0.978	0.977
		0.025	0.024	0.121	0.122	0.135	0.137	0.211	0.212
004	Δ_1	1.269	1.502	1.237	1.460	1.233	1.428	1.211	1.402
		1.026	1.029	1.040	1.042	1.042	1.047	1.051	1.052
		-0.126	-0.123	-0.004	-0.002	0.014	0.017	0.113	0.116
		-1.164	-1.160	-1.056	-1.055	-1.039	-1.032	-0.950	-0.947
	Δ_2	0.944	0.948	1.003	1.006	1.011	1.013	1.055	1.055
	$\Delta_{2'}$	0.646	0.650	0.757	0.759	0.773	0.776	0.858	0.860
	Δ_5	0.954	0.949	1.003	1.004	1.011	1.013	1.052	1.053
		0.006	0.006	0.103	0.104	0.118	0.118	0.196	0.196
006	Δ_1	1.413	1.693	1.376	1.626	1.371	1.607	1.340	1.557
		1.062	1.066	1.073	1.076	1.074	1.072	1.084	1.082
		-0.122	-0.122	-0.011	-0.009	0.006	0.011	0.100	0.103
		-1.168	-1.164	-1.052	-1.052	-1.035	-1.031	-0.944	-0.942
	Δ_2	0.981	0.982	1.033	1.035	1.040	1.041	1.078	1.079
	$\Delta_{2'}$	0.573	0.568	0.695	0.690	0.713	0.709	0.806	0.803
	Δ_5	1.038	1.033	1.078	1.074	1.084	1.080	1.113	1.109
		-0.003	-0.003	0.093	0.093	0.108	0.108	0.186	0.187
008	X_1	1.761	1.762	1.678	1.679	1.667	1.667	1.601	1.602
		1.057	1.054	1.070	1.068	1.072	1.071	1.084	1.081
		-1.180	-1.179	-1.057	-1.056	-1.039	-1.036	-0.944	-0.944
	X_2	0.997	0.996	1.047	1.047	1.053	1.053	1.089	1.089
	X_3	0.545	0.534	0.671	0.662	0.689	0.681	0.786	0.779
	$X_{4'}$	1.506	.....	1.475	.....	1.471	.....	1.444	.....
		-0.095	-0.101	0.005	0.001	0.020	0.016	0.108	0.105
	X_5	1.065	1.057	1.101	1.094	1.107	1.100	1.132	1.127
	$X_{5'}$	0.001	-0.005	0.093	0.091	0.107	0.105	0.186	0.184
048	W_1	1.835	1.833	1.746	1.744	1.734	1.732	1.660	1.656
		1.115	1.114	1.136	1.136	1.138	1.142	1.153	1.154
		-0.096	-0.087	0.025	0.031	0.043	0.048	0.138	0.142
	$W_{1'}$	1.066	1.057	1.102	1.094	1.107	1.100	1.133	1.127
	$W_{2'}$	1.044	1.044	1.068	1.067	1.071	1.073	1.089	1.094
		-1.144	-1.149	-1.035	-1.037	-1.019	-1.024	-0.933	-0.935
	W_3	1.719	.....	1.674	.....	1.667	.....	1.627	.....
		0.810	0.830	0.886	0.905	0.898	0.916	0.956	0.971
		-0.069	-0.062	0.035	0.039	0.050	0.053	0.137	0.139

Table 5.2 (continued)

$\vec{k}$		I		II		III		IV	
		APW	LCAO	APW	LCAO	APW	LCAO	APW	LCAO
022	Σ_1	1.132	1.305	1.101	1.260	1.098	1.250	1.088	1.211
		0.953	0.943	0.996	0.995	1.002	1.003	1.029	1.036
		0.875	0.873	0.943	0.942	0.953	0.951	1.003	1.002
		-0.065	-0.065	0.047	0.041	0.063	0.051	0.153	0.147
		-1.176	-1.178	-1.067	-1.064	-1.050	-1.045	-0.959	-0.957
	Σ_2	0.819	0.819	0.901	0.900	0.913	0.911	0.974	0.973
	Σ_3	1.961	.....	1.943	.....	1.939	.....	1.916	.....
		0.770	0.779	0.857	0.865	0.870	0.878	0.935	0.942
		0.010	0.011	0.109	0.110	0.123	0.124	0.202	0.202
	Σ_4	1.016	1.014	1.055	1.053	1.060	1.060	1.089	1.087
		-0.025	-0.022	0.086	0.088	0.102	0.104	0.188	0.190
044	Σ_1	1.407	1.723	1.374	1.650	1.370	1.631	1.341	1.571
		1.027	1.029	1.059	1.061	1.063	1.066	1.086	1.089
		0.928	0.931	0.978	0.984	0.986	0.991	1.023	1.030
		-0.162	-0.149	-0.034	-0.026	-0.015	-0.009	0.088	0.093
		-1.119	-1.120	-1.024	-1.025	-1.010	-1.012	-0.930	-0.931
	Σ_2	0.924	0.932	0.988	0.992	0.997	1.000	1.043	1.044
	Σ_3	1.796	.....	1.760	.....	1.754	.....	1.719	.....
		0.830	0.847	0.901	0.918	0.912	0.929	0.966	0.980
		-0.046	-0.038	0.059	0.062	0.074	0.076	0.160	0.161
	Σ_4	1.160	1.163	1.167	1.171	1.168	1.169	1.173	1.176
		-0.083	-0.090	0.041	0.037	0.058	0.057	0.154	0.153
066	K_1	1.790	1.805	1.718	1.717	1.706	1.709	1.638	1.633
		1.069	1.071	1.086	1.091	1.088	1.096	1.102	1.112
		0.696	0.708	0.792	0.803	0.806	0.817	0.880	0.889
		-0.092	-0.078	0.021	0.031	0.038	0.045	0.130	0.136
		-1.145	-1.150	-1.036	-1.038	-1.020	-1.024	-0.934	-0.936
	K_2	1.026	1.025	1.071	1.067	1.077	1.073	1.108	1.105
	K_3	1.610	.....	1.576	.....	1.571	.....	1.540	.....
		0.970	0.981	1.018	1.029	1.025	1.036	1.060	1.072
		-0.084	-0.081	0.019	0.020	0.034	0.035	0.122	0.122
	K_4	1.091	1.086	1.117	1.113	1.121	1.117	1.140	1.137
		-0.048	-0.051	0.062	0.059	0.078	0.076	0.166	0.165
222	Λ_1	1.159	1.408	1.125	1.349	1.121	1.335	1.097	1.288
		0.802	0.813	0.880	0.889	0.892	0.899	0.951	0.955
		-0.096	-0.103	0.019	0.011	0.036	0.027	0.129	0.122
		-1.154	-1.154	-1.052	-1.049	-1.036	-1.031	-0.950	-0.947
	Λ_3	1.026	1.025	1.063	1.062	1.068	1.068	1.096	1.094
		0.866	0.867	0.940	0.938	0.949	0.948	1.002	1.001
		-0.033	-0.031	0.079	0.080	0.095	0.095	0.183	0.183
444	L_1	1.772	1.773	1.689	1.690	1.677	1.678	1.607	1.610
		0.887	0.868	0.940	0.921	0.946	0.926	0.986	0.970
		-0.215	-0.215	-0.079	-0.077	-0.059	-0.056	0.051	0.052
	L_3	1.163	1.163	1.172	1.171	1.173	1.170	1.179	1.177
		0.972	0.966	1.022	1.018	1.029	1.025	1.065	1.062
		-0.091	-0.097	0.035	0.030	0.053	0.049	0.151	0.147
	$L_{2'}$	1.243	.....	1.251	.....	1.252	.....	1.256	.....
		-1.085	-1.085	-1.003	-1.005	-0.990	-0.997	-0.918	-0.921

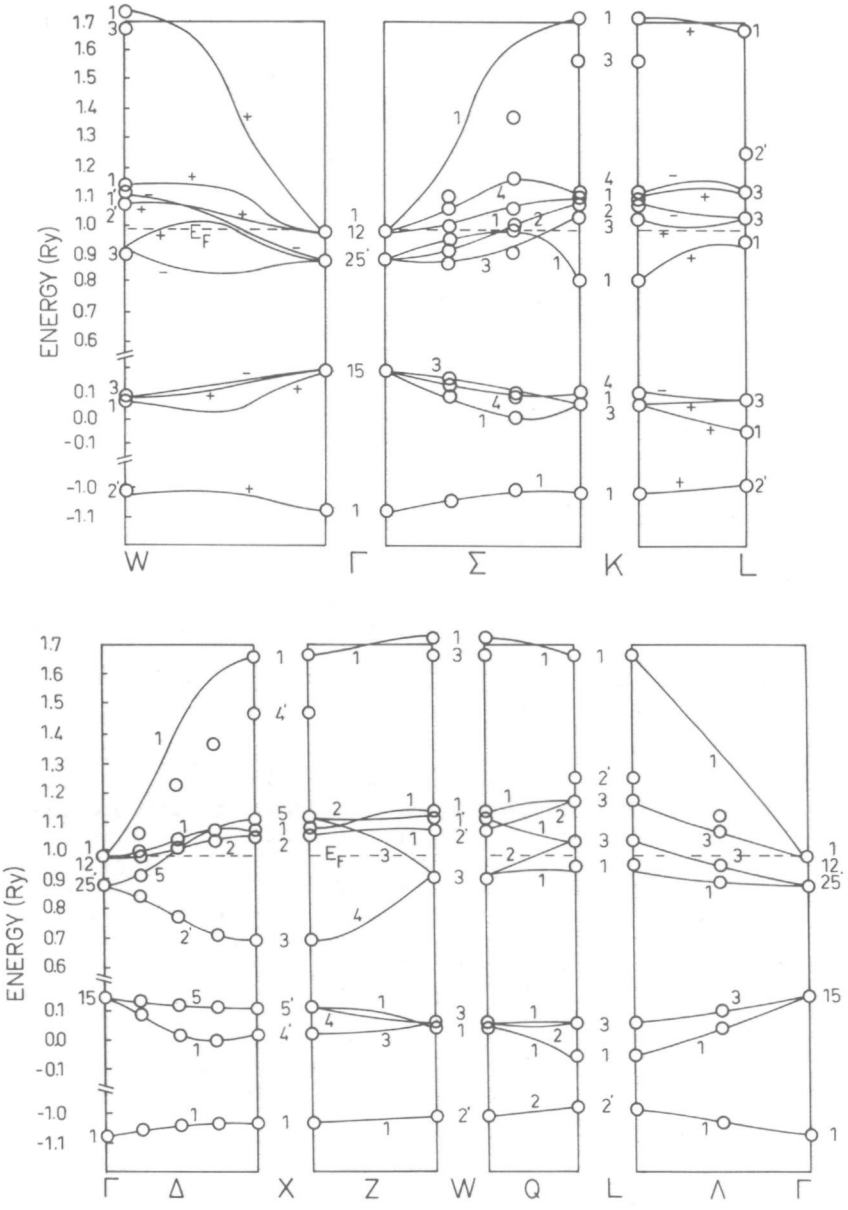

Fig. 5.1 The band structure of VO for a = 7.735 au. The circles indicate the APW eigenvalues, the lines correspond to the interpolated values.

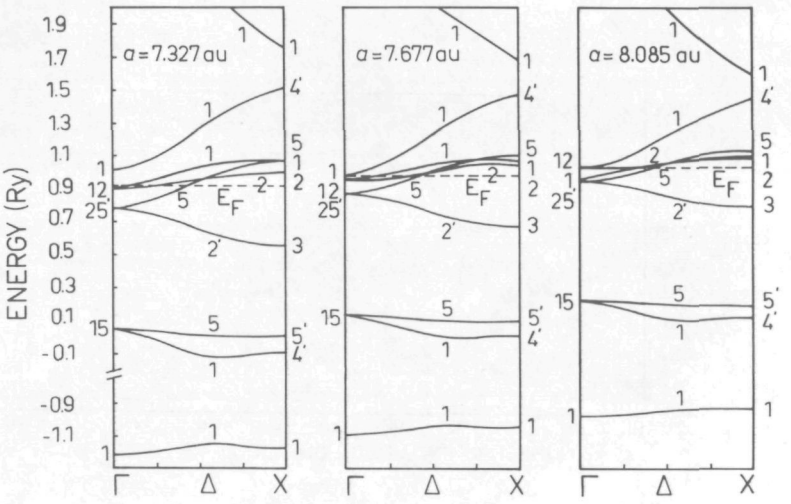

Fig. 5.2 Comparison between the band structures of VO for several lattice parameters.

relativistic way. Relativistic effects will have little influence, since vanadium and oxygen are small atoms. Inclusion of all relativistic effects except the spin-orbit coupling, shifts the vanadium 4s band roughly 0.005 Ry downwards, while the vanadium 3d band is about 0.005 Ry higher.

The inclusion of the non-muffin-tin potential in the form of the Fourier coefficients has a remarkable effect on the APW eigenvalues. It shifts the bottom of the vanadium 4s band as has been illustrated by figure 5.3 (a = 7.677 au).

5.4 THE LCAO INTERPOLATION SCHEME

The 89 APW eigenvalues, we have at our disposal, enable us to determine the 29 LCAO parameters by a least-squares method. The least-squares method is in fact an optimization problem, that is the minimum of the least-squares sum has to be sought. In this case the procedure of Marquardt (3) is preferable to other existing methods. The LCAO interpolation fits rather good the APW

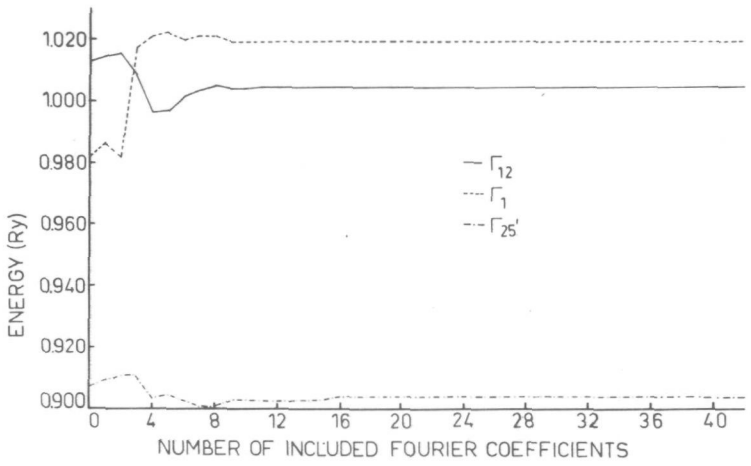

Fig. 5.3 The influence of the non-muffin-tin terms on the APW eigenvalues of VO at the Γ-point (a = 7.677 au).

eigenvalues. However the Δ_1, Σ_1 and Λ_1 states that belong to the vanadium 4s band, are hard to adapt. The corresponding weighing factors w_i have been given therefore the symbolic value 0.01 instead of 1.0. The bad adaptation of some states is mainly caused, we suppose, by the non-inclusion of the vanadium 4p basis functions. Further, we should realize that the vanadium 4s electron, due to its great distance to the nucleus, shows a plane wave character more than an atomic orbital character, which makes the application of the LCAO formalism difficult anyhow. On the other hand, we remark that vanadium 4s states, which do not admix with the vanadium 4p orbitals for symmetry reasons, like Γ_1, X_1, W_1 and L_1, are very well fitted.

The values of the LCAO parameters are shown in table 5.3. With the help of these LCAO parameters, it is possible to obtain the Fermi energy and the density of states, which are shown in figure 5.4. The Fermi energy and the errors of the LCAO interpolation scheme can be found in table 5.4.

The density of states and the Fermi energy E_F are deter-

Table 5.3

Transfer and overlap integrals of the LCAO interpolation scheme for VO. I, II, III and IV refer to the respectively lattice constants 7.327, 7.677, 7.735 and 8.085 au.

Cation-cation interactions	(Ry) I	II	III	IV
$E_{3z^2-r^2,3z^2-r^2}(000)$	0.9926	0.8502	0.8528	0.8829
$E_{3z^2-r^2,3z^2-r^2}(\frac{1}{2}\frac{1}{2}0)$	-0.0044	-0.0197	-0.0201	-0.0200
$E_{x^2-y^2,x^2-y^2}(\frac{1}{2}\frac{1}{2}0)$	-0.0112	0.0390	0.0399	0.0430
$E_{s_c,3z^2-r^2}(\frac{1}{2}\frac{1}{2}0)$	0.0064	0.0156	0.0259	0.0186
$E_{s_c,s_c}(000)$	1.5071	1.4731	1.3715	1.3950
$E_{s_c,s_c}(\frac{1}{2}\frac{1}{2}0)$	-0.0584	-0.0479	-0.0633	-0.0457
$E_{xy,3z^2-r^2}(\frac{1}{2}\frac{1}{2}0)$	0.0146	0.0171	0.0160	0.0130
$E_{s_c,xy}(\frac{1}{2}\frac{1}{2}0)$	-0.0426	-0.0318	-0.0298	-0.0222
$E_{xy,xy}(000)$	0.8535	0.9268	0.9377	0.9933
$E_{xy,xy}(\frac{1}{2}\frac{1}{2}0)$	-0.0509	-0.0418	-0.0405	-0.0334
$E_{xy,xy}(0\frac{1}{2}\frac{1}{2})$	0.0145	0.0122	0.0119	0.0100
$E_{xy,xz}(0\frac{1}{2}\frac{1}{2})$	0.0197	0.0162	0.0155	0.0127
Anion-anion interaction				
$E_{s_a,s_a}(000)$	-1.0851	-1.0045	-0.9969	-0.9211
$E_{s_a,s_a}(\frac{1}{2}\frac{1}{2}0)$	0.0031	0.0037	0.0067	0.0035
$E_{s_a,x}(\frac{1}{2}\frac{1}{2}0)$	0.0041	0.0003	-0.0070	0.0003
$E_{x,x}(000)$	-0.0186	0.0791	0.0937	0.1738
$E_{x,x}(\frac{1}{2}\frac{1}{2}0)$	0.0086	0.0082	0.0083	0.0073
$E_{x,x}(0\frac{1}{2}\frac{1}{2})$	-0.0035	-0.0029	-0.0029	-0.0026
$E_{x,y}(\frac{1}{2}\frac{1}{2}0)$	-0.0176	-0.0104	-0.0048	-0.0039
Cation-anion interactions				
$E_{s_a,3z^2-r^2}(00\frac{1}{2})$	-0.0641	0.1509	0.1237	0.1177
$E_{z,3z^2-r^2}(00\frac{1}{2})$	0.0023	-0.0027	-0.0388	0.0049
$E_{s_c,s_a}(\frac{1}{2}00)$	0.1049	0.0772	0.1154	0.0728
$E_{s_c,x}(\frac{1}{2}00)$	0.1927	0.1547	0.1291	0.1125
$E_{x,xy}(0\frac{1}{2}0)$	0.0463	0.0383	0.0389	0.0308
$S_{s_a,3z^2-r^2}(00\frac{1}{2})$	-0.0287	-0.0973	-0.1248	-0.1250
$S_{z,3z^2-r^2}(00\frac{1}{2})$	0.1642	0.2079	0.1722	0.1938
$S_{s_c,s_a}(\frac{1}{2}00)$	-0.0038	0.0107	-0.0235	0.0002
$S_{s_c,x}(\frac{1}{2}00)$	0.0024	-0.0057	-0.0414	-0.0284
$S_{x,xy}(0\frac{1}{2}0)$	-0.0499	-0.0417	-0.0385	-0.0312

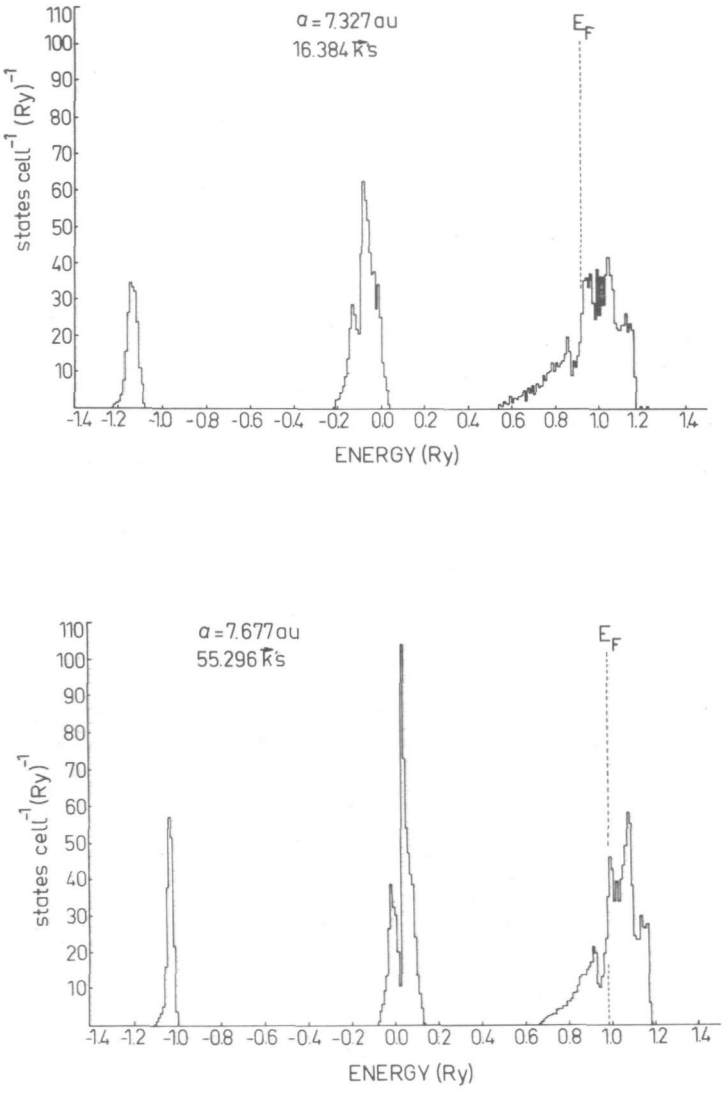

Fig. 5.4 The density of states and the Fermi energy E_F for several lattice parameters a of VO.

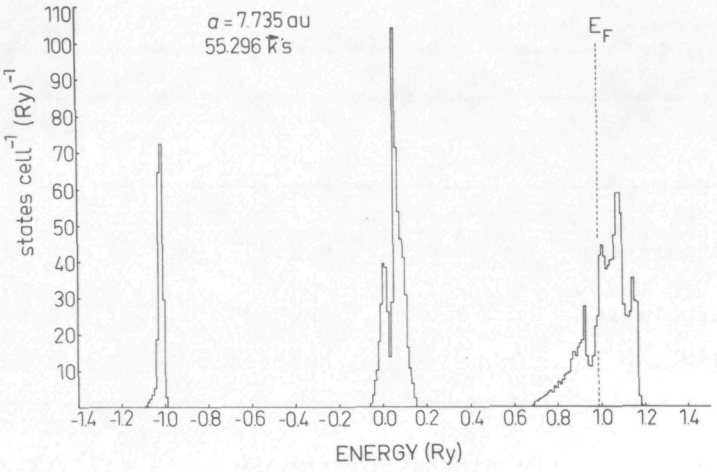

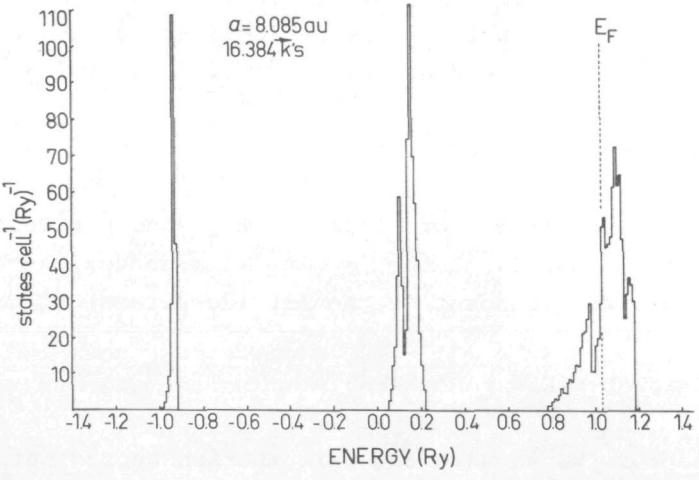

Fig. 5.4 (continued)

Table 5.4

Some energy parameters in the APW-LCAO calculation of VO.

	units	I	II	III	IV
Max error in the LCAO interpolation	Ry	0.0203	0.0190	0.0201	0.0163
Rms error in the LCAO interpolation	Ry	0.0064	0.0053	0.0057	0.0049
Fermi energy E_F	Ry	0.923	0.980	0.988	1.031

mined by a histogram technique. For the cases II and III, we have used thereby 55,296 $\vec{k}$-points, while for the less important cases I and IV only 16,384 $\vec{k}$-points are taken. In figure 5.4 we see how the density of states changes as a function of the lattice parameter a. One can ascertain that a small lattice parameter leads to a broad energy band.

The LCAO interpolation tells us further that the t_{2g} band is the broadest band with a bandwidth

$$W_{t_{2g}} = E(X_5) - E(X_3)$$

The e_g band is smaller and overlaps the t_{2g} band partially. The bottom of the e_g band is at the Γ-point in $\vec{k}$-space, the top of the e_g band varies dependent on the lattice parameter.

5.5 THE CRYSTAL-FIELD PARAMETERS

In chapter IV, we gave the perturbation approximation to determine the crystal-field parameters from the LCAO interpolation parameters. The values of these crystal-field parameters have been listed in table 5.5. The crystal-field parameter Δ decreases with an increasing lattice parameter.

To get an impression of the reliability of these values, we

Table 5.5

Crystal-field parameters for VO as calculated from the LCAO interpolation parameters. I, II, III and IV refer to the respectively lattice constants 7.327, 7.677, 7.735 and 8.085 au.

	units	I	II	III	IV
Δ_{s_a}	Ry	0.0037	0.1766	0.1718	0.1730
Δ_{σ}	Ry	0.1532	0.2506	0.2724	0.2337
Δ_{π}	Ry	0.0725	0.0559	0.0533	0.0373
Δ'_{s_c}	Ry	-0.0222	-0.0148	-0.0164	-0.0098
Δ''_{s_c}	Ry	-0.0010	-0.0047	-0.0155	-0.0081
Δ	Ry	0.1919	0.1141	0.1111	0.0752
Δ	cm^{-1}	21,060	12,520	12,190	8,259

compare them with the experimental results of V^{2+} in MgO, for the numerical value of Δ is mainly determined by the oxygen atoms that surround the central vanadium atom. Sturge (4) has found for Δ by optical experiments the value 13,200 cm^{-1}. Since MgO has a lattice distance a of 7.952 au, linear interpolation between our theoretical calculated Δ values results in a Δ value 9,747 cm^{-1} for V^{2+} in MgO.

Mattheiss (5) ascribed the fact that the numerical value of Δ is somewhat too small to the overestimate of the 2p-3d band gap. A reduction of this gap decreases the denominator of the second order perturbation theory approximation for the crystal-field parameters.

However, the derivation in paragraph 4.4 of the crystal-field parameter Δ as a function of the LCAO interpolation para-

meters is only an approximation. As discussed earlier, we have therefore also calculated the parameter Δ by using the LCOAO interpolation scheme of Slater and Koster (6) for the vanadium 3d band. In table 5.6 the LCOAO parameters are enumerated, where vanadium second-nearest-neighbour interactions have been included in the interpolation scheme. It is instructive to compare these results with those that can be obtained from the perturbation approximation as outlined in table 4.4. These results are listed in table 5.7. The LCOAO parameters, where even the vanadium third-nearest-neighbour interaction has been incorporated, are summarized in table 5.8. This shows us that the parameter Δ from table 5.6 is rather reliable. The relation between this crystal-field parameter Δ and the lattice distance a is illustrated by figure 5.5. Linear interpolation results in a Δ-value 12,600 cm^{-1} for V^{2+} in MgO. This value is in good agreement with the experimental data. It indicates at the same time that the correlation effects are small.

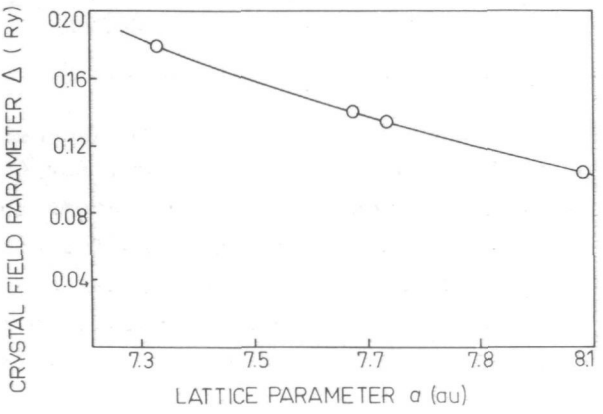

Fig. 5.5 Crystal-field parameter Δ as a function of the lattice constant a.

5.6 COMPARISON WITH OTHER CALCULATIONS

We have also executed an APW calculation under the same conditions as above, but with an α-value 2/3 (see paragraph 3.6) for the lattice constant a = 7.677 au. Using for α the value 2/3 in-

Table 5.6

LCOAO interpolation parameters, whereby the vanadium 3d functions are taken as the basis set. As far as the second neighbour interaction has been included.

Transfer Integral (Ry)	I	II	III	IV
$\varepsilon_{xy,xy}(000)$	0.8910	0.9545	0.9637	1.0112
$\varepsilon_{xy,xy}(\frac{1}{2}\frac{1}{2}0)$	-0.0510	-0.0419	-0.0405	-0.0334
$\varepsilon_{xy,xy}(0\frac{1}{2}\frac{1}{2})$	0.0148	0.0125	0.0122	0.0103
$\varepsilon_{xy,xz}(0\frac{1}{2}\frac{1}{2})$	0.0089	0.0084	0.0083	0.0077
$\varepsilon_{xy,xy}(100)$	-0.0095	-0.0068	-0.0064	-0.0043
$\varepsilon_{xy,xy}(001)$	-0.0001	-0.0006	-0.0005	-0.0007
$\varepsilon_{3z^2-r^2,3z^2-r^2}(000)$	1.0702	1.0942	1.0973	1.1145
$\varepsilon_{3z^2-r^2,3z^2-r^2}(\frac{1}{2}\frac{1}{2}0)$	-0.0058	-0.0063	-0.0063	-0.0070
$\varepsilon_{x^2-y^2,x^2-y^2}(\frac{1}{2}\frac{1}{2}0)$	-0.0111	-0.0069	-0.0063	-0.0038
$\varepsilon_{xy,3z^2-r^2}(\frac{1}{2}\frac{1}{2}0)$	0.0000	0.0000	0.0000	0.0000
$\varepsilon_{3z^2-r^2,3z^2-r^2}(001)$	-0.0257	-0.0201	-0.0193	-0.0149
$\varepsilon_{x^2-y^2,x^2-y^2}(001)$	-0.0018	-0.0023	-0.0024	-0.0032
Δ	0.1792	0.1396	0.1336	0.1033
rms error	0.0123	0.0119	0.0118	0.0136
max error	0.0409	0.0420	0.0419	0.0410

Table 5.7

The effective d-d interactions expressed in LCAO parameters by a perturbation theory approximation.

P. T. approximation (Ry)	I	II	III	IV
$E_{xy,xy}(000)+\frac{1}{2}(\Delta_\pi+\Delta'_{s_c})$	0.8787	0.9474	0.9562	1.0071
$E_{xy,xy}(\frac{1}{2}\frac{1}{2}0)$	-0.0509	-0.0418	-0.0405	-0.0334
$E_{xy,xy}(0\frac{1}{2}\frac{1}{2})$	0.0145	0.0122	0.0119	0.0100
$E_{xy,xz}(0\frac{1}{2}\frac{1}{2})-(\Delta_\pi+2\Delta'_{s_c})/8$	0.0162	0.0129	0.0129	0.0105
$E_{xy,xy}(100)-(\Delta_\pi+2\Delta'_{s_c})/8$	-0.0035	-0.0033	-0.0026	-0.0022
$E_{xy,xy}(001)$	0.0000	0.0000	0.0000	0.0000
$E_{3z^2-r^2,3z^2-r^2}(000)+\frac{1}{2}(\Delta_{s_a}+\Delta_\sigma+\Delta''_{s_c})$	1.0706	1.0615	1.0672	1.0822
$E_{3z^2-r^2,3z^2-r^2}(\frac{1}{2}\frac{1}{2}0)+(3\Delta_{s_a}+\Delta''_{s_c})/36$	-0.0041	-0.0051	-0.0062	-0.0058
$E_{x^2-y^2,x^2-y^2}(\frac{1}{2}\frac{1}{2}0)-(4\Delta_{s_a}+\Delta''_{s_c})/16$	-0.0121	-0.0049	-0.0021	0.0003
$E_{xy,3z^2-r^2}(\frac{1}{2}\frac{1}{2}0)-(3\Delta_\pi\Delta_\sigma)^{\frac{1}{2}}/12$	-0.0003	0.0000	-0.0014	-0.0005
$E_{3z^2-r^2,3z^2-r^2}(001)-(\Delta_\sigma-\Delta_{s_a})/6$	-0.0249	-0.0123	-0.0168	-0.0101
$E_{x^2-y^2,x^2-y^2}(001)$	0.0000	0.0000	0.0000	0.0000

Table 5.8

LCOAO interpolation parameters, whereby the vanadium 3d functions are taken as the basis set. As far as the third neighbour interaction has been included.

Transfer Integral (Ry)	I	II	III	IV
$\varepsilon_{xy,xy}(000)$	0.8903	0.9536	0.9628	1.0105
$\varepsilon_{xy,xy}(\frac{1}{2}\frac{1}{2}0)$	-0.0513	-0.0422	-0.0408	-0.0337
$\varepsilon_{xy,xy}(0\frac{1}{2}\frac{1}{2})$	0.0157	0.0132	0.0128	0.0108
$\varepsilon_{xy,xz}(0\frac{1}{2}\frac{1}{2})$	0.0096	0.0089	0.0088	0.0082
$\varepsilon_{xy,xy}(100)$	-0.0092	-0.0065	-0.0061	-0.0041
$\varepsilon_{xy,xy}(001)$	-0.0001	-0.0006	-0.0006	-0.0007
$\varepsilon_{xy,xy}(\frac{1}{2}\frac{1}{2}1)$	0.0006	0.0004	0.0004	0.0003
$\varepsilon_{xy,xy}(\frac{1}{2}1\frac{1}{2})$	-0.0009	-0.0006	-0.0006	-0.0006
$\varepsilon_{xy,xz}(\frac{1}{2}\frac{1}{2}1)$	0.0001	0.0000	-0.0001	-0.0001
$\varepsilon_{xy,xz}(1\frac{1}{2}\frac{1}{2})$	0.0015	0.0013	0.0012	0.0010
$\varepsilon_{3z^2-r^2,3z^2-r^2}(000)$	1.0699	1.0944	1.0975	1.1146
$\varepsilon_{3z^2-r^2,3z^2-r^2}(\frac{1}{2}\frac{1}{2}0)$	-0.0070	-0.0075	-0.0076	-0.0085
$\varepsilon_{x^2-y^2,x^2-y^2}(\frac{1}{2}\frac{1}{2}0)$	-0.0115	-0.0071	-0.0065	-0.0038
$\varepsilon_{xy,3z^2-r^2}(\frac{1}{2}\frac{1}{2}0)$	-0.0006	0.0000	0.0002	0.0007
$\varepsilon_{3z^2-r^2,3z^2-r^2}(001)$	-0.0259	-0.0204	-0.0196	-0.0152
$\varepsilon_{x^2-y^2,x^2-y^2}(001)$	-0.0015	-0.0020	-0.0021	-0.0028
$\varepsilon_{x^2-y^2,x^2-y^2}(\frac{1}{2}\frac{1}{2}1)$	0.0002	0.0001	0.0001	-0.0002
$\varepsilon_{3z^2-r^2,3z^2-r^2}(\frac{1}{2}\frac{1}{2}1)$	0.0014	0.0016	0.0017	0.0019
$\varepsilon_{xy,3z^2-r^2}(\frac{1}{2}\frac{1}{2}1)$	0.0005	0.0000	-0.0001	-0.0004
$\varepsilon_{xz,3z^2-r^2}(\frac{1}{2}\frac{1}{2}1)$	0.0016	0.0004	0.0003	0.0003
$\varepsilon_{xz,x^2-y^2}(\frac{1}{2}\frac{1}{2}1)$	0.0014	-0.0002	-0.0004	-0.0004
Δ	0.1795	0.1408	0.1347	0.1041
rms error	0.0094	0.0092	0.0092	0.0113
max error	0.0257	0.0252	0.0248	0.0212

stead of 1 results in a broader 3d band. The bandwidth of the t_{2g} band becomes now 0.519 Ry (compare: 0.432 Ry for $\alpha = 1$). So a smaller α promotes a broader 3d band. Another feature is the overlap of the 3d and 4s band: $E(\Gamma_1) - E(\Gamma_{12}) = -0.019$ Ry.

Mattheiss (5) has executed a similar calculation as we did for VO with a = 7.735 au (see figure 5.6). Only he has not in-

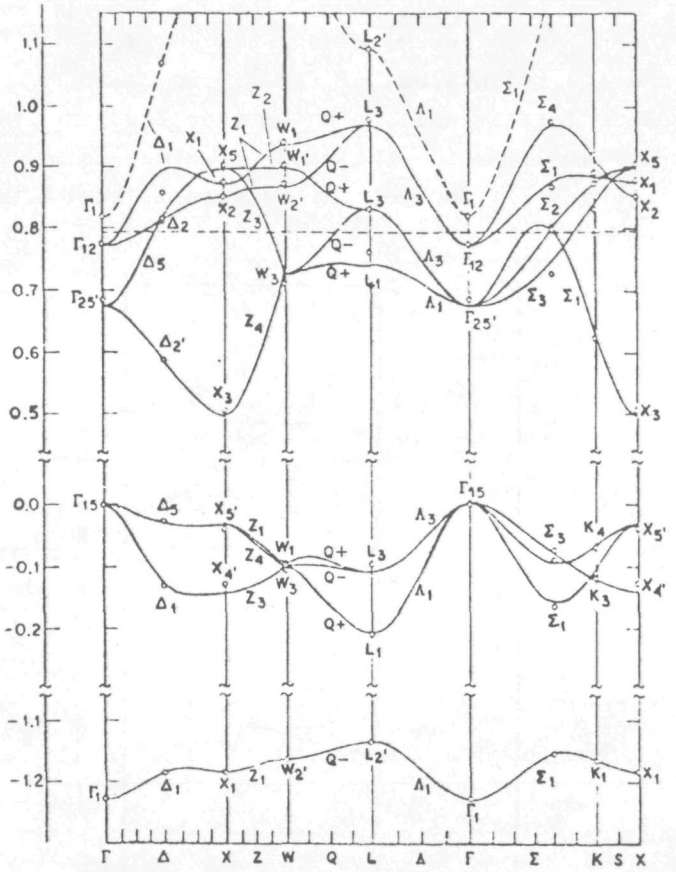

Fig. 5.6 The band structure of VO according to L.F. Mattheiss (5). The energy is expressed in Rydbergs.

cluded the vanadium 4s orbital in the interpolation scheme, while the transfer integrals are simplified to a two-centre approximation. It will be evident that not only our interpolation of the APW eigenvalues is more accurate, but also the Fermi energy E_F will be exacter. This is particularly relevant since at the

Γ-point the vanadium 4s state drops below the Fermi energy. Although our value, obtained for the crystal-field parameter Δ (0.1336 Ry), compares well with the value given by Mattheiss (Δ = 0.1332 Ry), our 3d bands are somewhat broader than those obtained by Mattheiss. We believe that the latter finding is a consequence of the inclusion of more atoms in obtaining the muffin-tin potential.

We will now pay attention to the work of Honig *et al.* (7), who have tried to fit the APW eigenvalues of fcc TiO as calculated by Ern and Switendick (8). It will be known that TiO has the same crystal structure as VO, while the band structure is almost identical (see figure 5.7). The general feature is that

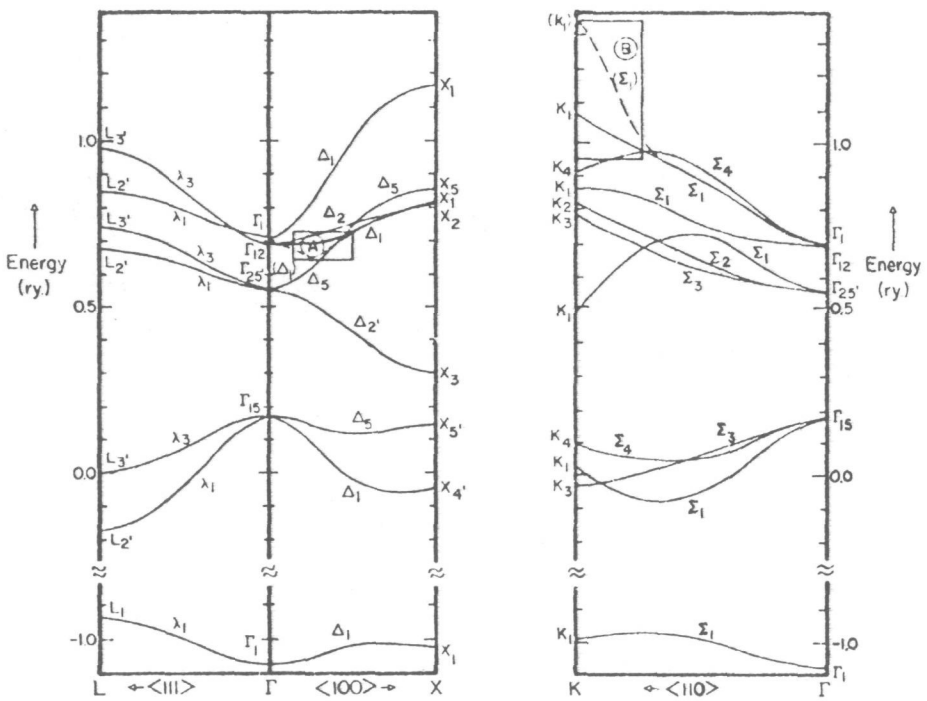

Fig. 5.7 The LCOAO interpolation of the APW eigenvalues of TiO. Large deviations occur in area A and B (ref. 7).

the d bands are somewhat broader, while there is more overlap between the titanium 4s and 3d band. They have adapted the APW eigenvalues with an LCOAO interpolation scheme, thereby taking the same basis functions as we do, with this difference that their basis functions are mutually orthogonal. The 24 independent transfer integrals are determined by the best fit to 38 eigenvalues. For two states, namely the K_1-state belonging to the titanium 4s band and the Δ_1-state related to the titanium 3d band, the LCOAO and APW eigenvalues show large deviations. This is particularly important because of the proximity of that Δ_1-state to the Fermi level. We have two objections to the followed procedure. We believe in the first place that too few APW eigenvalues are used in order to get reliable transfer integrals. Secondly, we don't think it is justified to give each state the same weight.

Mattheiss (5) has compared the band structure of the transition metal (mon)oxides with each other. It is equally interesting to make a comparison of VO with VN and VC. These last two mentioned compounds also have the NaCl structure. The lattice constants of VC and VN are respectively 7.903 and 7.801 au (9). On the ground of our band structure calculations, one would expect that because of the large lattice constants the 3d bands of VC and VN will be narrower than those of VO. On the other hand, carbon and nitrogen have a lower nuclear charge than oxygen, in consequence the 2p electrons will be less tightly bound. The 2p bands will therefore increase in energy going from VO via VN to VC. States belonging to the vanadium 3d band, which can admix with the 2p band for symmetry reasons will be pushed upwards. These conclusions are supported by calculations of Neckel *et al.* (1,10) on VC and VN (see figure 5.8 and 5.9). They establish that in VN the 2p band almost touches the 3d band. In VC these bands even overlap each other. The L_3 and Σ_4 states belonging to the 3d band of VC and VN have considerably higher energies than the comparable states in VO. This is caused, as mentioned above, by the influence of the oxygen 2p band.

In table 5.9 our transfer and overlap integrals are compared with those used in or obtained by other calculations. Norwood and

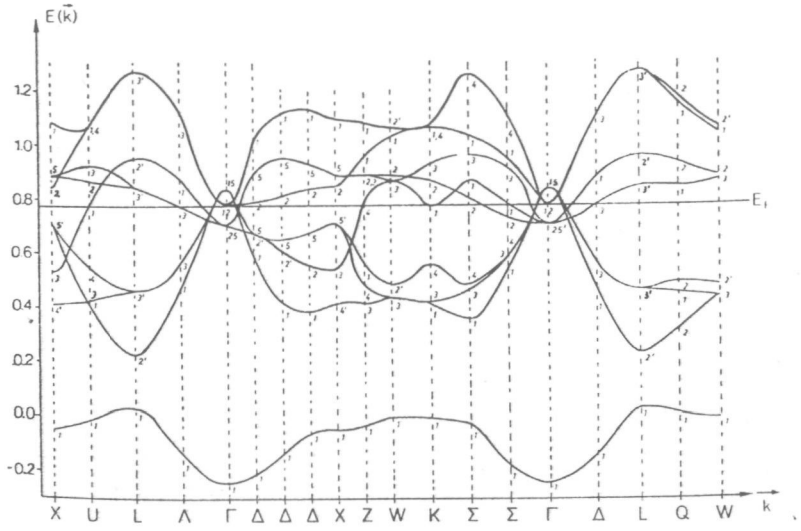

Fig. 5.8 The band structure of VC. The energy is expressed in Rydbergs (ref. 10).

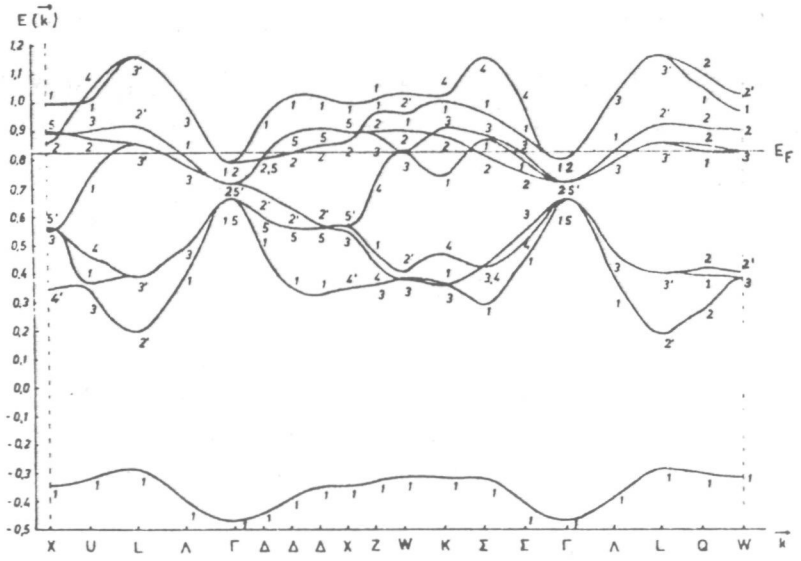

Fig. 5.9 The band structure of VN. The energy is expressed in Rydbergs (ref. 1).

Table 5.9

Comparison between the transfer and overlap integrals of the LCAO interpolation scheme with those of other calculations on VO.

	Norwood & Fry		Mattheiss		This work*	
	E	S	E	S	E	S
$3z^2-r^2, 3z^2-r^2$ (000)	-0.535	1.000	-0.426	1.000	-0.471	1.000
xy, xy (000)	-0.395	1.000	-0.395	1.000	-0.395	1.000
xy, $3z^2-r^2$ ($\frac{1}{2}\frac{1}{2}$0)	0.015	-0.128	0.021	0.000	0.017	0.000
s_a, $3z^2-r^2$ (00$\frac{1}{2}$)	-0.390	0.121	-0.222	0.056	0.289	-0.125
z, $3z^2-r^2$ (00$\frac{1}{2}$)	-0.289	0.109	-0.217	0.084	-0.266	0.172
x, xy (0$\frac{1}{2}$0)	0.173	-0.083	0.093	-0.033	0.090	-0.039
$3z^2-r^2, 3z^2-r^2$ ($\frac{1}{2}\frac{1}{2}$0)	-0.161	0.140	0.015	0.000	-0.020	0.000
x^2-y^2, x^2-y^2 ($\frac{1}{2}\frac{1}{2}$0)	0.088	-0.287	0.026	0.000	0.039	0.000
xy, xy ($\frac{1}{2}\frac{1}{2}$0)	-0.032	0.029	-0.039	0.000	-0.042	0.000
xy, xy (0$\frac{1}{2}\frac{1}{2}$)	0.020	-0.110	0.011	0.000	0.012	0.000
xy, xz (0$\frac{1}{2}\frac{1}{2}$)	0.033	-0.018	0.014	0.000	0.016	0.000
s_c, s_c (000)	-1.593	1.000	--	--	0.152	1.000
s_c, s_c ($\frac{1}{2}\frac{1}{2}$0)	-0.856	0.456	--	--	-0.048	0.000
s_a, s_a (000)	-2.399	1.000	-2.271	1.000	-2.326	1.000
x, x (000)	--	1.000	-1.187	1.000	-1.243	1.000
x, x ($\frac{1}{2}\frac{1}{2}$0)	0.037	-0.020	0.009	0.000	0.008	0.000
x, x (0$\frac{1}{2}\frac{1}{2}$)	-0.027	0.013	-0.005	0.000	-0.003	0.000
x, y ($\frac{1}{2}\frac{1}{2}$0)	0.083	-0.033	0.014	0.000	-0.010	0.000

* a = 7.735 au.

Fry (11) have calculated transfer and overlap integrals directly, thereby choosing for the lattice parameter the value 7.676 au. Mattheiss' work (5) has been mentioned earlier. He applied the

APW-LCAO method, as we have done, but in a less exact form. He has ascertained the value 7.735 au to the lattice constant. The energy levels are shifted to make comparison possible. The zero of energy for the LCAO parameters has been shifted so that the transfer integrals $E_{xy,xy}(000)$ have equal values. The assumed configuration for the three cases is $V(3d^4 4s^1)$ and $O(2p^4)$. The numerical agreement between the APW-LCAO results of Mattheiss and ours on the one hand and those of Norwood and Fry on the other hand is very bad.

The first six transfer and overlap integrals determine the positions of the e_g and t_{2g} band with regard to each other. Covalency effects are included here. The next two integrals are mainly responsable for the bandwidth of the e_g band, while the following three integrals determine the t_{2g} bandwidth. The remaining transfer and overlap integrals are less interesting, they are important for the vanadium 4s and the oxygen 2s and 2p band. The most striking deviation is that between our values for the transfer and overlap integrals $s_a, 3z^2-r^2(00\frac{1}{2})$ and those of the others authors. Even the signs have opposite values. The discrepancy might be linked to our introduction of the vanadium 4s orbitals. A second point is the remarkable value for the transfer integral $E_{s_c,s_c}(000)$ of Norwood and Fry. Considering that this integral defines the position of the vanadium 4s level, it is not to be expected that its value would be even lower than the corresponding values for the 3d levels of t_{2g} and e_g symmetry. Another fact that concerns Mattheiss' results and our work is the relative unimportance of the transfer integrals between the oxygen 2p orbitals $E_{x,x}(\frac{1}{2}\frac{1}{2}0)$, $E_{x,x}(0\frac{1}{2}\frac{1}{2})$ and $E_{x,y}(\frac{1}{2}\frac{1}{2}0)$. It can be advantageous to give these integrals the value zero and take other integrals as parameters to be adapted.

Comparing Mattheiss' and our results we see, as we have already notified that the largest deviation is for the integrals $E_{s_a,3z^2-r^2}(00\frac{1}{2})$ and $S_{s_a,3z^2-r^2}(00\frac{1}{2})$. The other integrals have the same order of magnitude. We believe that our values are better suited for the interpolation procedure, since Mattheiss has not used the three-centre integrals as inde-

pendent parameters, but has composed these integrals out of a two-centre approximation by the relations as outlined by Slater and Koster (6). We must stress again that the transfer and overlap integrals as used by Mattheiss and us have no direct physical reality. They should not match in detail the physically significant values of Norwood and Fry. Nevertheless it is interesting that a certain correspondence is still present.

Finally it may be mentioned, that Norwood and Fry's transfer and overlap integrals have been used in a direct tight-binding or LCAO calculation of the band structure of VO (see figure 5.10).

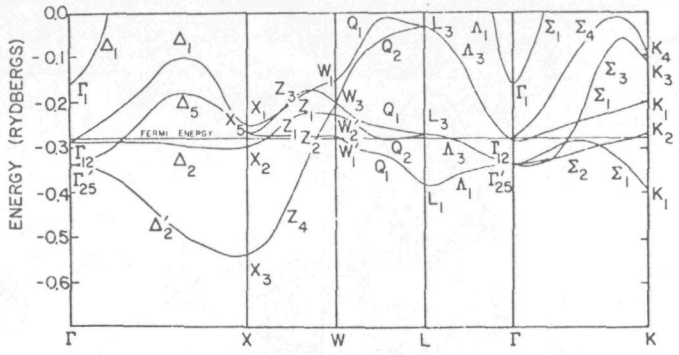

Fig. 5.10 The tight-binding calculation on VO. according to Norwood and Fry (11).

They find the best results for the configuration $V(3d^4 4s^1)$ and $O(2p^4)$. The bandwidth of the t_{2g} band is $(E(\Sigma_3)-E(X_3))$ that is about 0.5 Ry. The objection to their method is not the accuracy of their transfer and overlap integrals, but the inaccuracy of the ab-initio LCAO method. We have already noted in chapter IV that such LCAO methods fail for valence s or p electrons, which happens in VO.

Recently, still another band structure calculation on VO has been published by Tewari (12). He has used the ionic configuration $\{V(3d^3 4s^1), O(2p^5)\}$. He probably has not included the non-flatness of the muffin-tin potential outside the spheres by Fourier coefficients. He also establish an overlap of the vanadium 3d and 4s band (see figure 5.11).

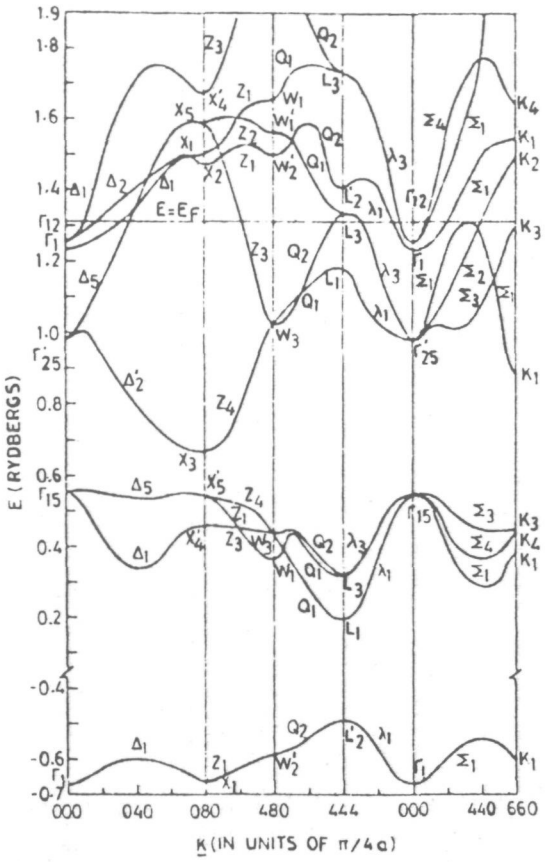

Fig. 5.11 The band structure of VO according to Tewari (12).

REFERENCES

1. NECKEL A., *Int. Conference on Solid Compounds of Transition Elements*, University of Geneva, Switserland, April 9-13, 1973
2. SLATER J.C. and WOOD J.H., *Int. J. Quant. Chem.* 4, 3 (1971)
3. MARQUARDT D.W., *J. Soc. Ind. Appl. Math.* 11, 431 (1963)
4. STURGE M.D., *Phys. Rev.* 130, 639 (1963)
5. MATTHEISS L.F., *Phys. Rev.* B 5, 290 (1972)
6. SLATER J.C. and KOSTER G.F., *Phys. Rev.* 94, 1498 (1954)
7. HONIG J.M., WAHNSIEDLER W.E. and DIMMOCK J.O., *J. Solid State Chem.* 5, 452 (1972)
8. ERN V. and SWITENDICK A.C., *Phys. Rev.* 137, A1927 (1965)
9. WYCKOFF R.W.G., *Crystal Structures*, Vol. 1, Wiley & Sons, New York (1964)
10. NECKEL A., RASTL P., WEINBERGER P. and MECHTLER R., *Theoret. Chim. Acta* 24, 170 (1972)

11. NORWOOD T.E. and FRY J.L., *Phys. Rev.* B 2, 472 (1970)
12. TEWARI S., *Solid State Commun.* 11, 1139 (1972)

CHAPTER VI - CONCLUSIONS AND EVALUATION

In the preceding chapters we have presented the results of APW-LCAO calculations on the band structure of VO as a function of the lattice parameter a. A crucial point is, in retrospect, whether the one-electron approach, inherent to this type of calculations, is justified or not. Hence it is important to evaluate the effect of interelectron correlation interactions, for instance by application of the criteria of Mott and Hubbard.

According to Anderson's (1) estimate, the average Coulomb repulsion energy U between the 3d electrons in a V^{2+} ion equals 0.43 Ry. According to the results of this thesis, the t_{2g} bandwidth of the crystals corresponding to the lattice parameters a = 7.327 to a = 8.085 au are found to be 0.523, 0.432, 0.419 and 0.347 Ry, respectively. According to Mott and Hubbard (paragraph 2.2) in the first case the band is sufficiently broad to justify a one-electron approximation, the second case is a borderline case, while in the last two cases correlation effects would lead to band splitting. Apart from all complications due to the orbital degeneracies of the d electrons, which make the Mott and Hubbard approximations dubious, we know further that for the two greater values of the lattice parameters the vanadium 4s band is partially occupied. Heine and Mattheiss (2) have suggested that in such a case the fast vanadium 4s electrons screen the vanadium 3d electrons. The effect of U is thus reduced, which means that the APW-LCAO calculation might be a better justified alternative for all four considered lattice parameters.

Similar conclusions then would hold for the other band structure calculations as reviewed in chapter V. Further, we have established in the same chapter that diminishing the constant α of the exchange potential from 1 to $\frac{2}{3}$ results in a broader d band, again decreasing the relative importance of correlation effects.

In our view, band structure calculations on VO performed thus far would agree with VO being a metallic type conductor with a relatively narrow band. The effective mass of the charge carriers then is expected to be great, the magnetism would be a rel-

atively large Pauli paramagnetism. Very good reasons for the occurrence of a semiconductor-metal transition upon increase of temperature cannot be obtained from the band calculations as presented.

Turning to a second model for a semiconductor-metal transition, the approach of Falicov and Kimball (3) allows of a simple description for VO. Based on the observations of Morin (4) sensible data would be obtained for the separation of the localized levels and the bottom of the conduction band, $\Delta = 0.018$ Ry, and for the electron-hole attraction parameter $G = 0.017$ Ry. The localized states according to Falicov and Kimball should be the $^4A_2$ ground terms of the V^{2+} ions. Excitation of electrons from this state to for instance $^4T_2$ would lead to delocalized electronic states effectively forming a conduction band. For comparison with the parameter Δ, it should be mentioned that the $^4A_2 \rightarrow {}^4T_2$ excitation energy of the V^{2+} ion in an octahedral crystal field of oxygen anions is 0.12 Ry. The quantity G should be compared with the ionization energy of $2V^{2+} \rightarrow V^{+} + V^{3+}$. As mentioned earlier this corresponds to 0.43 Ry. Apparently substantial screening effects have to be accounted for. The model of Falicov and Kimball does not give ab-initio information about Δ and G. Hence, predictions whether or not a semiconductor-metal transition is to be expected are not possible. Considering the susceptibility measurements, as have been summarized in chapter I, the model of Falicov and Kimball does not lead to consistent results. With localized V^{2+} states, magnetic moments of 3.87 μ_B per ion would be expected. Although a temperature dependent susceptibility is observed, the magnetic moments per ion, 0.69 μ_B, are considerably smaller than the spin-only value. We believe, therefore, that only a small percentage of electrons is in localized states. It is well possible, that this is due to the presence of about 15% vacancies, which cause a so-called Anderson localization (5), which has no great influence on the band structure.

Finally, we turn to the possibility of a semiconductor-metal transition in VO according to the principles of Goodenough. Goodenough (6) conjectures that upon deformation of the cubic crys-

tal field, possibly added by correlation effects, the t_{2g} band will split in two subbands separated by a narrow energy gap. We establish that in the limit of localized electrons the ground state will be a $^4A_2$ state. Further, every primitive cell of VO contains one formula unit, hence there are three valence electrons per cell. The $^4A_2$ state is an orbital singulet state, hence will be quite insensitive to Jahn-Teller distortions. Moreover an odd number of valence electrons would never lead to a complete filled band. We extrapolate this conclusion to the VO crystal with collective electrons. In principle, a degeneracy could be introduced by doubling the cell. Such a double cell then would contain an even number of electrons. By reducing the degeneracy, a completely filled lower band could be split off, or talking in magnetic terms, pairs of interacting V-ions could be formed. However, we do not see a simple way how such a structure could arise out of a cubic fcc lattice. Further, it has been remarked by Mattheiss (7) already that in an fcc structure the overlap of t_{2g} and e_g bands is an essential feature of the band structure belonging to this symmetry. This overlap will not be removed easily by lowering the symmetry.

The arguments given here do not apply to V_2O_3 and VO_2. Thus Goodenough's approach may explain very well the semiconductor-metal transition of these compounds. It may not be accidental that the experimental detection of the semiconductor-metal transition of these compounds is completely straightforward, while there is still considerable experimental uncertainty of the existence of such a transition for VO.

Quite recently very interesting band structure calculations for VO_2 have been published by Caruthers *et al.* (8), both for the distorted and the undistorted lattice. They established that the change in crystal symmetry can result in a splitting of a partially filled d band into subbands, which are either completely full or completely empty. They thus explain the semiconductor-metal transition of VO_2 in the sense of Goodenough.

All in all, we come to the conclusion that there is no single reason why VO, as to the feasibility of a semiconductor-metal

transition, should be placed in the same category as V_2O_3 and VO_2. The APW-LCAO calculations ascribe a predominant metallic character to VO, where a relative broad d band is formed by overlap of vanadium t_{2g} and e_g bands. The physical properties may be influenced to a certain extent by a slight overlap of these d bands with the vanadium 4s band. If semiconductor-metal transitions occur, they probably would be of a Mott type. It is doubtful whether computations of the type given in this thesis could ever be made sufficiently accurate to decide whether a transition will occur or not. Not only the accuracy is limited due to restrictions of the size of the set of basis functions and to the number of adjustable parameters for the interpolation, but more serious is the basic inadequacy of all models introducing correlation effects thus far.

Most promising is the method introduced by the Hubbard Hamiltonian. But in applying this Hamiltonian to the discussion of compounds of transition metal ions, the interatomic d electron interactions still are insufficiently taken into account. Not only variations of oxidation states and correlation therein have to be considered, but also the spin-governed exchange interactions. The multitude of spin configurations in a d band is far too great for effective handling. Ways should be found to isolate from this multitude the analogues of the ground term of the isolated ion and the states most easily derived therefrom by interatomic excitation or spin inversion of individual d electrons. Only then the possibility will arise to discuss side by side the changes in electric and magnetic properties, which occur upon semiconductor-metal transitions in compounds of transition metal ions.

REFERENCES

1. ANDERSON P.W., *Phys. Rev.* 115, 2 (1959)
2. HEINE V. and MATTHEISS L.F., *J. Phys. C* 4, L191 (1971)
3. FALICOV L.M. and KIMBALL J.C., *Phys. Rev. Letters* 22, 997 (1969)
4. MORIN F.J., *Phys. Rev. Letters* 3, 34 (1959)
5. MOTT N.F., *Phil. Mag.* 24, 935 (1971)
6. GOODENOUGH J.B., *Czech. J. Phys.* B 17, 304 (1967)
7. MATTHEISS L.F., *Phys. Rev.* B 5, 306 (1973)
8. CARUTHERS E, KLEINMAN L. and ZHANG H.J., *Phys. Rev.* B 7, 3753 (1973)

APPENDIX I - DETERMINATION OF THE STARTING VALUES OF THE LCAO INTERPOLATION SCHEME

The least-squares problem

$$\sum_{i=1}^{m} w_i (E_i - \varepsilon_i)^2 \rightarrow \text{minimum} \quad (m=89)$$

we have to solve is very sensitive to the starting values of the parameters we have to determine. Most of the ε_i-values are dependent on these parameters in a non-linear way. Moreover there are difficulties in connecting together the corresponding ε_i's and E_i's. For example: the 10 by 10 secular determinant that we have to solve for a certain symmetry point in $\vec{k}$-space can be transformed in some subdeterminants for symmetry reasons. For the 1 by 1 and 2 by 2 subdeterminants it is possible to indicate which of the ε_i's and E_i's are connected together. This is no longer possible if the determinants have an order 3 or higher. In order to meet both problems at the same time we have concentrated on the n coefficients of the "characteristic polynomial" of the n by n subdeterminant instead of the n roots. If the n eigenvalues ε_i are the solutions of the equation

$$\varepsilon^n + A_1 \varepsilon^{(n-1)} + \ldots + A_{n-1}\varepsilon + A_n = 0$$

(the A's are functions of the matrix elements), the coefficients of the "characteristic polynomial" are the following:

$$A_1 = -(\varepsilon_1 + \varepsilon_2 + \ldots + \varepsilon_n),$$

$$A_2 = (\varepsilon_1\varepsilon_2 + \varepsilon_1\varepsilon_3 + \ldots + \varepsilon_1\varepsilon_n + \varepsilon_2\varepsilon_3 + \ldots + \varepsilon_{n-1}\varepsilon_n),$$

$$A_n = (-1)^n \sum (\varepsilon_1\varepsilon_2 \ldots \varepsilon_n).$$

The E_i's are rearranged in the same way:

$$E_i' = (-1)^i \sum (E_1 E_2 \ldots E_i).$$

After this transformation the part of the least-squares sum corresponding to the n by n subdeterminant now reads

$$\sum_{i=j}^{j+n} w_i' (E_i' - A_i)^2.$$

The new created least-squares problem is rather insensitive to starting values. We took them all equal to 0.1. The resulting values for the parameters are used as starting values for the original least-squares problem.

APPENDIX II - SHORT DESCRIPTION OF THE USED COMPUTER PROGRAMS

The program that calculates the atomic charge density and potential by the Dirac-Slater method, is the relativistic program HEX of D.A.Liberman, J.T.Waber and D.T.Cromer[1]. We have adapted the program, which was written in Fortran IV for a CDC 6600, to our IBM 360/65 computer. The only really programmatical modification we made, was a better integration method in subroutine ADLINT, which has as a consequence that the wave functions are better normalized. The atomic charge densities are punched on cards, which can be used for the muffin-tin potential code.

The muffin-tin potential program MTPOT has been based on the code of T.L.Loucks as has been described in his book: *"Augmented Plane-Wave Method"*. We have not only made this program more accurate (e.g. by improving the subroutine for the α-Löwdin expansion), but we have also extended it considerably. So the constant Coulomb potential has been calculated by the integral method of F.S.Ham and B.Segall in subroutine CSTPT. Fourier coefficients of the potential between the atoms are calculated in subroutine FCOEFF. The output of the program consists of values for the radii of the muffin-tin spheres, the constant potential, the muffin-tin potential within the spheres and the Fourier coefficients of the potential between the spheres.

The subroutine for the solution of the Dirac equations in the spheres, DLGKAP, was obtained from D.D.Koelling[2]. His program calculates straightway the relativistic analogue of the logarithmic derivatives of the radial wave function at the muffin-tin spheres as a function of the energy E in a similar way as described by T.L.Loucks.

The most important computer program of our project is the (S)APW computer code according to Switendick, which we received from D.A.Papaconstantopoulos[3]. The program was written in Fortran V for an Univac 1108 computer. It can only calculate cubic structures. We have adapted the program for our computer and we have added one subroutine viz. V1MEP, which supplies the

appropriate Fourier coefficients when they are necessary. A noteworthy fact is, that we have used this program for a more extended basis set than used hitherto, since former users have only calculated metals, which need a relatively small basis set,

The LCAO interpolation scheme consists of three codes, which have been programmed in the course of this work. The first program STARTVAL performs the minimization or least-squares problem to calculate the starting values as has been outlined in Appendix I. For the minimization, the procedure DAPODMIN (S.A.Lill, *The Computer Journal* 13, 111 (1970)) is used, which searches a minimum according to the Davidon method. With the help of the starting values the final least-squares problem is executed by program MINLEIGV. With the so obtained numerical values for the transfer and overlap integrals, the LCAO eigenvalues can be obtained for a dense network in $\vec{k}$-space by program INTERPOLATE. Moreover the density of states and the Fermi energy E_F are calculated. The last two programs make use of the diagonalization procedure for complex matrices COMEIG (P.J.Eberlein, *Num. Math.* 14, 232 (1970)). This last procedure has been published in the Algol language. This is one of the main reasons, why this last category of three computer programs has been written in Algol 60. Program MINLEIGV uses the minimization procedure MARQUARDT, according to D.W.Marquardt (*J. Soc. Ind. Appl. Math.* 11, 431 (1963)), provided to us by Mr.C.J.Peters. This procedure is especially appropriate to optimization problems with many variables.

[1]We thank Dr.D.A.Liberman from the Los Alamos Scientific Laboratory, Los Alamos, California, USA for the relativistic self-consistent field program HEX for atoms and ions.

[2]We are grateful to Dr.D.D.Koelling from Northwestern University, Evanston, Illinois, USA for the subroutine DLGKAP.

[3]Our heartfelt thanks are expressed to Dr.D.A.Papaconstantopoulos from George Mason University, Fairfax, Virginia, USA for the SAPW program.

[4]We express our thanks to Mr.C.J.Peters of the Laboratory of Inorganic and General Chemistry for the procedure according to D.W.Marquardt.

SAMENVATTING

Metaal-halfgeleider overgangen, met de daarbij vaak gepaard gaande magnetische overgangen, hebben de laatste jaren in de literatuur veel aandacht gekregen. De groep van vanadiumoxiden (er zijn meerdere stoichiometrische samenstellingen bekend) neemt hierbij een belangrijke plaats in.

Veel kwalitatieve uitleggingen zijn er reeds gegeven om de overgangen te kunnen begrijpen. Sinds de komst van de computers is men in het begin van de jaren vijftig begonnen met een basis te leggen voor de kwantitatieve bepaling van de electronenniveaus in een kristal. Hierdoor kan een helderder inzicht verkregen worden in de metaal-halfgeleider overgangen.

In dit proefschrift zijn bandberekeningen uitgevoerd voor vanadiummonoxide. De keuze van deze verbinding, die een keukenzout kristalstruktuur heeft, is voornamelijk gedaan vanwege de hoge symmetrie en het lage aantal atomen per primitieve cel. Dit vereenvoudigt de ab-initio berekening nl. aanzienlijk.

De gebruikte berekeningen zijn uitgevoerd met de APW-LCAO methode. De APW methode wordt gebruikt om de energieniveaus voor enkele punten in de $\vec{k}$-ruimte met een hoge symmetrie te bepalen. De LCAO methode, waarbij als basisset de 3d en 4s Bloch orbitals van vanadium, en de 2s en 2p Bloch orbitals van zuurstof worden gebruikt, fungeert als een interpolatieschema ter bepaling van de energieniveaus voor de overige $\vec{k}$-punten.

Al onze berekeningen zijn uitgevoerd op de IBM 360/65 computer van het rekencentrum aan de Technische Hogeschool Delft. Sommige programma's zijn van andere onderzoekers verkregen en aangepast aan de voornoemde computer, terwijl andere programma's in de loop van het onderzoek zelf zijn ontwikkeld.

Om bij te dragen tot de discussie over de eventuele metaal-halfgeleider overgang van VO, is er een bandstruktuurberekening uitgevoerd voor vier verschillende roosterparameters.

De LCAO interpolatiemethode heeft ons tevens in staat gesteld om de kristalveld parameter Δ te berekenen en te vergelijken met die van het overeenkomstig gesitueerde V^{2+} in MgO.